Response to the anonymous reviews of "Sediment phosphorus speciation and mobility under dynamic redox conditions"

We thank both reviewers for their careful consideration and thorough review of our manuscript. Their comments and criticisms have allowed us to significantly improve the quality and clarity of the manuscript in its revised form. As you will see from the marked up manuscript and the table of changes below, we have made substantial revisions to the original submission in response to the reviewers concerns and suggestions. We have addressed all of the concerns highlighted by the reviewers and have made numerous additional changes to improve the readability, structure and technical content of our manuscript.

Briefly we have:

1. Re-written large sections of the manuscript, particularly emphasizing the aims of the study and novelty of the work, which we accept were not well expressed in the first iteration of the manuscript. We have also added a much more detailed discussion of the reactions occurring during the reactor experiment and within the sequential extraction procedure.
2. Included an additional Table, as requested by reviewer 2, to clarify the sequential extraction procedure used.
3. Calculated saturation indices for major Fe, S, Ca and P minerals using PHREEQC.
4. Included the additional data requested by both reviewers, within the manuscript and supplementary information.
5. Modified Figures 2, 3, 4 and 6.

A full list of changes is detailed in the table below:

Line number	**Changes made and rationale**
Line 15	Emphasize that our experiments deal with the reactions occurring within shallow sediment rather than directly at the SWI
Lines 21-23	Additional sentence to emphasize the breadth of data presented within the manuscript and one of the key novel contributions (mass balanced redistribution of P within solid and aqueous phases).
Lines 26-28	Provided more detail regarding the redistribution of P within the solid phase (key finding of the manuscript), without over interpretation of the extracted fractions.
Lines 29-31	Added the key results of the ^{31}P NMR analyses to the abstract to highlight that the paper is mostly about cycling of inorganic P species rather than organic-P.
Lines 34-36	Re-write of the concluding section of the abstract to better reflect the key conclusions of the study.
Line 67	Changed reference list to reflect the original study by Einsele.

Lines 72-76	New short section to highlight the common accumulation of polyphosphate in sediments, particularly under oscillating redox conditions.
Lines 80-94	Brief section added, at the request of reviewer 1, to discuss the key processes coupling the cycles of Fe, S, C and P.
Lines 95-99	Brief section added to highlight the novelty of laboratory experiments, which reflect dynamic, fluctuating natural environments.
Lines 102-107	Re-write of the key aims of the study more appropriate to the study design and to better reflect the novel findings
Lines 115-135	Field site and sampling section – Several parts restructured and nested sentences re-written to improve readability.
Line 140	Statement about sediment elemental concentrations from cores removed as this data is not shown (data lost).
Line 142-143	Details of software used for phase ID and quantitative phase analysis is now provided.
Lines 181-184	Statement added to explain the choice of reactor conditions e.g. temperature, dark etc
Lines 184-189	Re-written section to improve readability
Lines 210-212	Re-phrase to clarify that SEDEX extractions were performed on a time series from the reactor experiment rather than a depth profile.
Lines 218-228	Section re-written in more detail to explain the modifications made to the SEDEX method and to reference the new table.
Lines 233-235	New statement explaining how saturation indices were calculated.
Line 237	New statement to clarify that time series ^{31}P NMR data was collected from reactor samples.
Lines 278-279	Re-written sentence for clarity.
Lines 321-325	Re-written to provide more detailed information on pH trends within the reactor and referencing the data, which is now provided in Figure 3.
Lines 325-326	Inclusion of ionic strength data.
Line 326-330	Re-write to clarify which field conditions the reactor is replicating.
Lines 343-345	New statement regarding the effect of the reactor experiment on the biogeochemical function of the sediment.
Lines 348-351	Section moved from methods as suggested by reviewer 2.
Lines 355-358	New statement regarding the results of the thermodynamic model.
Line 378	New reference to Figure 3 added to the reactor pH data.
Lines 389-390	New statement to highlight the availability of all aqueous data in the supporting information.
Lines 392-394	New statement clarifying the relevance that the total extraction matches the sum of the sequential extracts.
Lines 396-401	New discussion about the stability and variability of different P fractions to highlight which fractions are involved in P redistribution during redox cycling.

Lines 411-423	New discussion about the content of the P_{Ex} fraction, how it compares to previous studies and the reaction mechanisms likely causing changes to P_{Ex} concentration over time.
Lines 424-430	Additional discussion about the probable content of the P_{Hum} fraction, how it compares to other common extractions and the rationale for its inclusion.
Lines 431-445	Re-written previous discussion on the content of the P_{Hum} fraction and comparison to similar commonly used extractions.
Lines 446-468	Re-written section.
Lines 469-476	New discussion on the reaction mechanisms causing release and immobilization of P from and to the P_{Hum} fraction.
Lines 477-483	New discussion of the P_{Fe} fraction – content and reaction mechanisms.
Lines 484-488	New discussion on the stability of the remaining P fractions.
Lines 494-495	Highlighting availability of solid phase chemistry data in the supporting information.
Lines 508-510	Inclusion of results from thermodynamic model.
Lines 521 and 526	References to Figure 6 added.
Lines 529-530	Additional information regarding the interpretation of the enzyme activities.
Lines 534-536	Additional statement to highlight the novelty of the enzyme activity results.
Lines 549-551	
Lines 551-555	Acknowledgement of the importance of degradation of P-diesters during analysis.
Lines 564-565	Additional link made between the ^{31}P NMR results and the sequential extraction results.
Lines 590-598	Re-write to be a) less specific about WWTPs, b) acknowledge the limits to the reactor experiment at predicting field scale response.
Lines 610-611	Added acknowledgements to people whose contribution should have been acknowledged in the first version of the manuscript.
Table 1	New table detailing the full sequential extraction scheme used.
Figure 2	We have added the depth interval used in the reactor experiment.
Figure 3	We have removed inconsistencies and improved clarity in the axis labels.
Figure 4	We have removed the 2^{nd} axis showing mg P L^{-1} for consistency.
Figure 6	We have added a statement explaining the absence of polyphosphate on the pie charts and increased the size of the text as suggested.
Supplementary Material	Full tabulated time series data for the reactor experiment is now provided.

Sediment phosphorus speciation and mobility under dynamic redox conditions

Chris T. Parsons[*1], *Fereidoun Rezanezhad*[1], *David W. O'Connell*[1,2], *Philippe Van Cappellen*[1]

[1]Ecohydrology Research Group and The Wate r Institute, University of Waterloo, 200 University Avenue West, Waterloo, Ontario, Canada.

[2]Department of Civil, Structural and Environmental Engineering, Trinity College Dublin, College Green, Museum Building, Dublin 2, Ireland.

[*]Corresponding author: Chris.Parsons@uwaterloo.ca

KEYWORDS: phosphorus, eutrophication, internal loading, redox cycling, bioturbation

ABSTRACT

Anthropogenic nutrient enrichment has caused phosphorus (P) accumulation in many freshwater sediments, raising concerns that internal loading from legacy P may delay the recovery of aquatic ecosystems suffering from eutrophication. Benthic recycling of P strongly depends on the redox regime within surficial sediment. In many shallow environments, redox conditions tend to be highly dynamic as a result of, among others, bioturbation by macrofauna, root activity,

Chris Parsons 2017-5-4 14:25
Deleted: at the sediment-water interface (SWI

Chris Parsons 2017-5-4 14:25
Deleted:)

Chris Parsons 2017-4-30 02:18
Deleted: that,

Chris Parsons 2017-4-30 02:18
Deleted: i

Chris Parsons 2017-4-30 02:19
Deleted: t

Chris Parsons 2017-4-30 02:19
Deleted: s

sediment resuspension and seasonal variations in bottom water oxygen (O_2) concentrations. To gain insight into the mobility and biogeochemistry of P under fluctuating redox conditions, a suspension of sediment from a hyper-eutrophic freshwater marsh was exposed to alternating 7-day periods of purging with air and nitrogen gas (N_2), for a total duration of 74 days in a bioreactor system. We present comprehensive data time series of bulk aqueous and solid phase chemistry, solid phase phosphorus speciation and hydrolytic enzyme activities demonstrating the mass balanced redistribution of P in sediment during redox cycling. Aqueous phosphate concentrations remained low (~2.5 μM) under oxic conditions, due to sorption to Iron(III)-oxyhydroxides. During anoxic periods, once nitrate was depleted, the reductive dissolution of Iron(III)-oxyhydroxides released P. However, only 4.5% of the released P accumulated in solution while the rest was redistributed between the $MgCl_2$ and $NaHCO_3$ extractable fractions of the solid phase. Thus, under the short redox fluctuations imposed in the experiments, P remobilization to the aqueous phase remained relatively limited. Orthophosphate predominated at all times during the experiment in both the solid and aqueous phase. Combined P monoesters and diesters accounted for between 9 and 16% of sediment particulate P. Phosphatase activities up to 2.4 mmol h^{-1} kg^{-1} indicated the potential for rapid mineralization of organic-P (P_o), in particular during periods of aeration when the activity of phosphomonoesterases was 37% higher than under N_2 sparging. The results emphasize that the magnitude and timing of internal P loading during periods of anoxia are dependent on both P redistribution within sediments and bottom water nitrate concentrations.

Chris Parsons 2017-4-30 02:20
Deleted: At the start of each anoxic period, algal necromass was added to simulate the deposition of fresh autochtonous organic matter.

Chris Parsons 2017-4-30 02:11
Moved down [5]: Phosphatase activities up to 2.4 mmol h^{-1} kg^{-1} indicated the potential for rapid mineralization of added organic-P (P_o), in particular during the periods of aeration when the activity of phosphomonoesterases was up to 37% higher than under N_2 sparging.

Chris Parsons 2017-5-5 10:25
Deleted: Fe

Chris Parsons 2017-4-25 10:10
Deleted: /Mn

Chris Parsons 2017-5-5 10:25
Deleted: Fe

Chris Parsons 2017-4-25 10:12
Deleted: /Mn

Chris Parsons 2017-4-25 10:17
Formatted: Subscript

Chris Parsons 2017-4-25 10:17
Formatted: Subscript

Chris Parsons 2017-4-25 10:15
Deleted: among the particulate phases, including the humic fraction.

Chris Parsons 2017-4-30 02:20
Deleted: relatively

Chris Parsons 2017-4-30 02:20
Deleted: -term

Chris Parsons 2017-4-30 02:21
Deleted: and poly-phosphate did not accumulate.

Chris Parsons 2017-4-30 02:14
Deleted:

Chris Parsons 2017-4-30 02:11
Moved (insertion) [5]

Chris Parsons 2017-5-4 14:30
Deleted: added

Chris Parsons 2017-5-4 16:18
Deleted: the

Chris Parsons 2017-4-30 10:47
Deleted: up to

Chris Parsons 2017-4-25 10:19
Deleted: also

Chris Parsons 2017-5-4 14:32
Deleted: e

Chris Parsons 2017-4-25 10:20
Deleted: important

Chris Parsons 2017-4-25 10:20
Deleted: control bottom water nitrate ... [1]

Chris Parsons 2017-5-4 16:19
Formatted: BD_Abstract

Keywords:

^{31}P NMR, sequential extractions, coupled biogeochemical cycling, phosphorus, iron, sulfur, redox oscillation, redox fluctuation, bioreactor, internal loading

INTRODUCTION

It is widely recognized that accelerated eutrophication of freshwater aquatic environments is caused primarily by anthropogenic increases to dissolved phosphorus (P) concentrations in surface water (Smith and Schindler, 2009). Rapid cultural eutrophication of oligo or mesotrophic lacustrine and palustrine systems is often attributed to increased external P loadings originating in agricultural run-off or waste water treatment plant (WWTP) effluent. The resultant excessive algal growth negatively impacts aquatic ecosystems and economic activity (Pretty et al., 2003), as well as increasing the risk of infectious diseases (Chun et al., 2013). Strategies to mitigate eutrophication have aimed to reduce point source and diffuse external phosphorus loadings by instituting agricultural best management practices in the surrounding watershed (McLaughlin and Pike, 2014; Sharpley et al., 1994), limiting P inputs to domestic waste water (Corazza and Tironi, 2011) and upgrading WWTPs (Mallin et al., 2005). However, internal loading of P, from sediments to surface water, remains poorly quantified in many systems, and is often the largest source of error in hydrodynamic and ecological phosphorus models (Kim et al., 2013). Early diagenesis and mineralogical removal of labile autochthonous organic phosphorus (P_o) from solution is a complex process and is poorly understood in highly dynamic systems despite exerting a strong influence on the magnitude and timing of internal P loading. This is

Chris Parsons 2017-4-25 10:29
Deleted: may exert on internal P loading in eutrophic environments.

Chris Parsons 2017-5-4 16:18
Deleted:

Chris Parsons 2017-5-4 16:18
Deleted: ... [2]

Chris Parsons 2017-4-25 11:46
Deleted: and

particularly true in shallow lakes and wetlands due to the high sediment surface area to water column depth ratio (Søndergaard et al., 2003).

As policy and infrastructure improvements continue in order to mitigate external P inputs to aquatic systems, the relative importance of internal P loads from legacy P in sediments to overall P budgets in eutrophic systems is likely to increase (Reddy et al., 2011).

It has been widely demonstrated through laboratory and field investigations, particularly in seasonally anoxic lakes, that sustained anoxic conditions induced by water column stratification, typically result in greater P mobility, and correspondingly higher water column P concentrations (D. Krom and A. Berner, 1981; Einsele, 1936; Hongve, 1997; Katsev et al., 2006; Mortimer, 1941, 1971; Penn et al., 2000). The microbially mediated reductive dissolution of iron(III) oxyhydroxides or iron(III) phosphate during sustained periods of anoxia at the sediment water interface (SWI) has long been considered the main mechanism responsible for P release under anoxic conditions e.g. (Bonneville et al., 2004; Hyacinthe and Van Cappellen, 2004). More recently, considerable microbial polyphosphate accumulation and release in response to alternating oxic-anoxic conditions at the SWI in lacustrine environments has also been shown to occur (Gächter et al., 1988; Gächter and Meyer, 1993; Hupfer et al., 2007; Sannigrahi and Ingall, 2005). In some cases this accumulation of polyphosphate by the microbial community may account for 10% of total phosphorus (Hupfer et al., 2007).

However, redox conditions in shallow, heavily bioturbated sediments are more spatially and temporally variable than in seasonally anoxic lakes (Aller, 1994; Gorham and Boyce, 1989) resulting in short term redox oscillations even with continuous oxia at the SWI.

Additionally, the coupled biogeochemical cycles of other redox sensitive elements such as sulfur and carbon have been shown to play important and complex roles in phosphorus mobility

Unknown
Field Code Changed

Chris Parsons 2017-4-25 10:46
Deleted: (D. Krom and A. Berner, 1981; Hongve, 1997; Katsev et al., 2006; Mortimer, 1971, 1941; Penn et al., 2000)

Chris Parsons 2017-4-27 10:11
Deleted: is often

Chris Parsons 2017-4-27 10:11
Deleted: to be the

Chris Parsons 2017-4-27 09:51
Deleted:

Chris Parsons 2017-4-27 14:42
Deleted:

Chris Parsons 2017-4-25 10:44
Deleted: , such as sulfur (Gächter and Müller, 2003) and carbon (Joshi et al., 2015; Katsev et al., 2006)

(Gächter and Müller, 2003; Joshi et al., 2015; O'Connell et al., 2015). For example, high bottom water sulfate concentrations have been shown to increase aqueous P in sediments by decreasing the permanent mineralogical removal of P within vivianite [$Fe_3(PO_4)_{2(s)}$] and by decreasing the abundance of iron(III) oxyhydroxides near to the SWI (Caraco et al., 1989). This is due to the scavenging of iron during the formation of iron sulfide minerals within sediment during diagenesis (Gächter and Müller, 2003). Carbon cycling also exerts considerable control over phosphorus mobility within sediment. The stoichiometry of freshly deposited organic matter (OM) in eutrophic water bodies approaches that of primary production i.e. ~C_{106}:N_{16}:P (Berner, 1977). Appreciable P may therefore be released to the aqueous phase when organic carbon is mineralized during microbial respiration of oxygen, nitrate, ferric iron or sulfate. In addition to driving N, Fe and S cycling, mineralization of organic carbon and concomitant P release has, in some places, been shown to be the primary mechanism controlling phosphorus mobility at the SWI (Joshi et al., 2015).

Core incubations and in-situ flux chambers frequently examine the effects of anoxia on P mobility from sediments but the effects of repetitive redox oscillations are rarely investigated in a controlled setting (Frohne et al., 2011; Matisoff et al., 2016; Nürnberg, 1988; Thompson et al., 2006). Consequently, the cumulative and reversible effects of oxic-anoxic cycling, on P distribution, speciation and mobility within sediments is poorly understood.

The aim of this study is to elucidate the microbial and geochemical mechanisms of in sediment phosphorus cycling and release associated with commonly occurring short redox fluctuations (days) in surficial sediments in shallow eutrophic environments. Particularly, we aimed to; 1) Quantify the redistribution of P between aqueous and mineral sediment pools during fluctuating redox conditions, 2) Determine if the activity of hydrolytic phosphatase enzymes acting on P_o

Unknown
Field Code Changed

Chris Parsons 2017-4-25 10:46
Deleted: (O'Connell et al., 2015)

Chris Parsons 2017-4-27 10:50
Formatted: Subscript

Chris Parsons 2017-4-27 10:50
Formatted: Subscript

Chris Parsons 2017-4-25 10:46
Deleted: Degradation of P_o can be slow below the SWI in lakes (Reitzel et al., 2007), occurring on timescales of years (Ahlgren et al., 2005) resulting in the accumulation and burial of P_o in sediments of hyper eutrophic lakes. P accumulation within microbial biomass in surface sediments has also been highlighted (Hupfer et al., 2008, 1995; Turner et al., 2006) as has long term P_o retention in tropical wetland sediments (Turner et al., 2006)

Chris Parsons 2017-4-27 13:13
Deleted: however the effects of near surface redox oscillations on P_o retention are not well understood.

Chris Parsons 2017-4-29 16:06
Deleted: at the SWI

Chris Parsons 2017-4-30 02:29
Deleted: determine if

Chris Parsons 2017-4-27 15:30
Deleted:

Chris Parsons 2017-4-27 16:15
Formatted: Not Highlight

Chris Parsons 2017-4-27 16:15
Formatted: Not Highlight

Chris Parsons 2017-4-27 15:30
Deleted: Polyphosphate cycling was observable within marsh sediments under redox oscillating conditions as has been shown in WWTP communities (Fu et al., 2009; Hupfer et al., 2007)

Chris Parsons 2017-4-27 16:15
Formatted: Not Highlight

Chris Parsons 2017-4-27 15:32
Deleted: .

Chris Parsons 2017-4-27 15:41
Deleted: The accumulation of autochthonous P_o species from algal necromass was an important P immobilizing process in an example hyper-eutrophic shallow wetland system 3)

Chris Parsons 2017-4-27 15:38
Deleted: Rates of P_o degradation

Chris Parsons 2017-4-27 16:15
Formatted: Not Highlight

Chris Parsons 2017-4-27 16:15
Formatted: Subscript, Not Highlight

were influenced by redox conditions, 3) Assess if the proportions of orthophosphate, P_o, and polyphosphate varied systematically with redox conditions and 4) Ascertain if P mobilization/immobilization mechanisms were reversible or cumulative.

We conducted controlled bioreactor experiments using sediment suspensions, designed to reproduce cyclic redox conditions analogous to those occurring in nature (Aller, .1994, 2004). A combination of aqueous chemistry, sediment sequential extractions (Ruttenberg, 1992), ^{31}P NMR spectroscopy (Cade-Menun, 2005) and extra-cellular enzyme assays (Deng et al., 2013) were used to produce a comprehensive dataset describing bulk chemistry, microbial and mineralogical controls on P mobility and speciation during redox oscillations.

METHODS

Field site and sampling

Surface sediment (0-12 cm), sediment cores (34 cm long, 10 cm diameter), overlying water and green filamentous algae (GFA) were collected on September 5, 2013 from West Pond in Cootes Paradise Marsh (43.26979N, 79.92899W) following established guidelines (U.S. EPA, 9/99). Cootes Paradise is a hyper-eutrophic, coastal freshwater marsh, which drains into Lake Ontario via Hamilton Harbour (see Figure 1A-1C). The marsh system suffered severe degradation due to rapid urbanization, population growth and nutrient loadings in the 20th century (Chow-Fraser et al., 1998). West Pond in particular received extremely high external P loads from the Dundas WWTP for several decades prior to the installation of sand filters in 1987 (Painter et al., 1991). The addition of sand filters, and other improvements, decreased P loadings from the WWTP from 45 kg P day^{-1} in the early 1970's (Semkin et al., 1976) to 4.5 kg P day^{-1} in the 1980s (Chow-Fraser et al., 1998) and 2.59 kg P day^{-1} in 2011 (Routledge, 2012). However, high

Chris Parsons 2017-4-27 16:01
Deleted: were a) affected by redox conditions

Chris Parsons 2017-4-27 15:43
Deleted:

Chris Parsons 2017-4-27 16:15
Formatted: Not Highlight

Chris Parsons 2017-4-27 16:15
Formatted: Not Highlight

Chris Parsons 2017-4-27 16:15
Formatted: Not Highlight

Chris Parsons 2017-4-27 16:15
Formatted: Not Highlight

Chris Parsons 2017-4-27 16:15
Formatted: Not Highlight

Chris Parsons 2017-4-27 16:15
Formatted: Not Highlight

Chris Parsons 2017-4-27 16:15
Formatted: Not Highlight

Chris Parsons 2017-4-27 15:43
Deleted: and b) comparable to those reported in deeper lake environments.

Chris Parsons 2017-4-26 16:34
Formatted: Highlight

Unknown
Field Code Changed

Chris Parsons 2017-4-25 10:46
Deleted: (Aller, 2004, 1994)

Chris Parsons 2017-4-25 11:56
Deleted: (cations, anions, dissolved organic carbon (DOC), SRP)

Chris Parsons 2017-4-30 11:00
Formatted: Superscript

Chris Parsons 2017-4-25 11:56
Deleted: (modified SEDEX protocol and TP), spectroscopy (solution ^{31}P NMR)

Chris Parsons 2017-4-25 11:56
Deleted: , using 4-methylumbelliferyl (MUF) tagged substrates,

Chris Parsons 2017-4-27 15:58
Deleted: evaluate

Chris Parsons 2017-4-27 16:00
Deleted: reactor experiments

Chris Parsons 2017-4-30 12:53
Deleted: **Methods**

Chris Parsons 2017-4-25 12:09
Deleted: , and particularly West Pond,

Chris Parsons 2017-4-25 12:09
Deleted: Sand filters were introduced to the Dundas WWTP, which flows into West Pond, in 1987 to decrease P loading, but prior to this ... [3]

Chris Parsons 2017-4-25 12:10
Deleted: further

external P loads resulted in accumulation of legacy P in West Pond sediments with total phosphorus concentrations reaching 200 μmol g^{-1} by the 1980's (Theysmeyer et al., 1999). Consequently, dredging was conducted in 1999 in an attempt to remediate the areas most affected by growth of green filamentous algae (Bowman and Theysmeyer, 2014).

Despite these restoration efforts and decreases to the external P load, pervasive growth of GFA during the summer persists in parts of Cootes Paradise (Figure 1A). Cyanobacteria are not commonly observed at this location, potentially due to the high N:P ratios often associated with WWTP which utilize tertiary P removal treatment (Conley et al., 2009; Stumm and Morgan, 1996).

Sediment characterization

Sediment cores were sliced every 3 cm, homogenized and characterized with bulk sediment samples prior to bioreactor experiments. Organic carbon and carbonate depth profiles were determined by thermo-gravimetric analysis (TGA-Q500, TA Instruments Q500) (Pallasser et al., 2013). Further elemental concentrations of Al(100), Ca(20), Fe(3), Mn(1) and P(2) were determined by ashing and acidic dissolution (HCl) followed by Inductively Coupled Plasma Optical Emission Spectrometry (ICP-OES, Thermo Scientific iCAP 6300). Method detection limits (MDL) in μg L^{-1} are shown in brackets. Water content and bulk density (ρ_b) of the sliced sediment core were determined gravimetrically after oven drying (Gardner, 1986). Identification and quantification of crystalline mineralogy was determined by powder X-ray diffraction (XRD) (Empyrean Diffractometer and Highscore Plus software Ver. 3.0e, PANalytical). The density of benthic macro-invertebrates was also quantified after sieving two additional 7.5 cm diameter, 18 cm deep cores through 500 µm mesh.

Chris Parsons 2017-4-25 12:13
Deleted:

Chris Parsons 2017-4-25 12:28
Deleted: However, high legacy P concentrations in sediment (up to 6200 μg g^{-1}) in the 1980's (Theysmeyer et al., 1999) resulted in dredging in order to remediate the most affected areas in 1999 in an attempt to reduce harmful green filamentous algae blooms

Chris Parsons 2017-4-25 12:09
Formatted: Font:12 pt

Chris Parsons 2017-4-30 11:02
Deleted: ,

Chris Parsons 2017-4-30 11:02
Deleted: , including West Pond

Chris Parsons 2017-5-4 11:29
Deleted: with

Chris Parsons 2017-4-30 11:02
Deleted: fractions

Chris Parsons 2017-4-25 13:06
Deleted: composition

Chris Parsons 2017-4-25 13:05
Deleted: (e.g. total phosphorus (TP))

Chris Parsons 2017-4-25 13:07
Deleted:

Chris Parsons 2017-4-25 13:06
Deleted: as

Chris Parsons 2017-4-25 13:08
Deleted:

Chris Parsons 2017-4-30 11:03
Deleted: Crystalline mineralogy phase

Chris Parsons 2017-4-30 11:03
Deleted: i

Chris Parsons 2017-4-30 11:03
Deleted: were

Chris Parsons 2017-4-25 13:12
Deleted: ,

Chris Parsons 2017-4-30 11:05
Deleted: by counting

Bioreactor experiment and redox oscillation procedure

An initial, concentrated, sediment suspension of approximately 500 g L^{-1} (dry weight equivalent) was prepared from freshly sampled sediment (0-12 cm) and filtered overlying water (< 0.45 μm). Surface water was used, rather than distilled water, to provide background ionic strength and avoid osmotic shock to the microbial community. The concentrated suspension was stirred vigorously for 5 minutes then passed through a < 500 µm stainless steel sieve to remove larger solid organic material and macro-invertebrates. This procedure was repeated until a homogeneous suspension was achieved. The dry weight was then re-determined, and the sieved solution was diluted with filtered surface water to a final concentration of 247 ± 2 g L^{-1}. The resulting suspension was transferred to a bioreactor system (Applikon Biotechnology) after Thompson et al (2006) and Parsons et al (2013). In addition to affording precise temperature control and continuous logging of temperature, redox potential (E_h) and pH, the system offers significant advancements over previous designs (Thompson 2006, Guo 2007, Parsons 2013). The E_h, pH and dissolved oxygen (DO) were measured using a combined autoclavable Mettler Toledo InPro 3253i/SG open-junction electrode and an AppliSens Low drift polarographic sensor. The InPro electrode system, using a common reference electrode, was chosen to help avoid potential interference between two electrodes in close proximity. A multi parameter transmitter was used to display current pH, E_h and temperature, to automatically temperature correct pH values and to adjust measured E_h to the standard hydrogen electrode (SHE). DO was calibrated using 100% saturation in air (approximately 0.2905 atm) and 0% saturation in N_2 at constant sparging of 30 ml min^{-1}

The suspension was stirred continuously and sparged with 30 mL min^{-1} air for 11 days to equilibrate prior to the redox oscillation procedure. During the 11-day oxic equilibration period,

Chris Parsons 2017-4-30 02:34
Deleted: (Thompson et al., 2006)

Unknown
Field Code Changed

Chris Parsons 2017-4-30 02:34
Deleted: (Parsons et al., 2013)

Unknown
Field Code Changed

Chris Parsons 2017-5-4 11:30
Deleted: Dissolved oxygen (

Chris Parsons 2017-5-4 11:30
Deleted:)

Chris Parsons 2017-5-4 14:08
Deleted:

297 CO_2 emissions were monitored in the reactor exhaust gas using an IR sensor (Applikon
298 Biotechnology).

299 Subsequently, redox potential (E_h) variation was induced by the modulation of sparging gases
300 (30 ml min^{-1}) between N_2:CO_2 and O_2:N_2:CO_2. The suspension was subjected to five cycles of
301 anoxia (7 days) and oxia (7 days) at constant temperature (25°C) in the dark, while recording E_h,
302 pH, DO and temperature data. The suspension was sampled on days 1, 3, 5 and 7 of each half-
303 cycle. To separate solid and aqueous components from the sediment suspension, syringe
304 extracted samples (15 ml) were centrifuged at 5000 rpm for 20 minutes and the supernatant
305 filtered through 0.45 µm polypropylene membrane filters prior to all aqueous analysis. For
306 samples taken during anoxic half cycles, centrifugation, filtering and subsampling were
307 performed in an anoxic glove box (N_2:H_2 97:3%, O_2 < 1 ppmv). Time periods were chosen to be
308 representative of short temporal fluctuations to redox conditions experienced by surficial
309 sediments (Aller, 1994; Nikolausz et al., 2008; Parsons et al., 2013). Similarly, the temperature
310 and dark conditions were chosen to reflect those measured in surficial sediment during summer
311 months at the field site. Summer conditions were chosen as this is when maximum bioturbation,
312 microbial activity and OM input are expected within the sediment. Similar, long-running batch
313 reactor experiments using soil or sediment have previously experienced a slowdown of metabolic
314 processes due to depletion of labile organic carbon (Parsons et al., 2013). Therefore, gaseous
315 carbon and nitrogen losses from the reactor were balanced by the addition of 3 g of freeze dried,
316 ground, GFA to the suspension at the onset of each anoxic cycle. The amount of algae added was
317 determined based on CO_2 production from the reactor during the initial 11 day oxic period.

Chris Parsons 2017-5-5 11:03
Deleted: N_2:CO_2

Chris Parsons 2017-5-4 00:28
Deleted: 3

Chris Parsons 2017-5-4 00:28
Deleted: 7

Chris Parsons 2017-4-30 02:36
Deleted: reducing

Chris Parsons 2017-4-25 12:35
Moved (insertion) [1]

Chris Parsons 2017-4-25 12:36
Deleted: .To avoid unrealistically high depletion of labile organic matter (OM) not replaced by primary productivity during the experiment,

Chris Parsons 2017-4-25 12:39
Deleted: were added to the suspension

Chris Parsons 2017-4-25 12:40
Deleted: the

Chris Parsons 2017-5-4 11:37
Deleted: , to balance gaseous carbon and nitrogen losses due to microbial metabolism and avoid depletion of labile organic carbon, which often results in a slowdown of metabolic processes in laboratory based soil and sediment experiments

Chris Parsons 2017-4-25 12:35
Moved up [1]: (Parsons et al., 2013).

Chris Parsons 2017-4-25 12:40
Formatted: Font:Times New Roman

Aqueous phase methods

All reagents used were of analytical grade from Fluka, Sigma-Aldrich or Merck unless stated otherwise and were prepared with 18.2 MΩ cm^{-1} water (Millipore). Total dissolved Na (70), K(100), Ca(20), Mg(0.5), Mn(1), Fe(3), Al(100), P (2), Si (15) and S (15) concentrations (MDL in μg L^{-1}, in brackets) were determined by ICP-OES (Thermo Scientific iCAP 6300) after filtration (< 0.45 μm) and acidification with HNO_3 to < pH 2. Matrix-matched standards were used for all calibrations and NIST validated multi-elemental solutions were used as controls. SRP concentrations were determined by the molybdenum blue/ascorbic acid method on a LaChat QuickChem 8500 flow injection analyzer system (*4500-P E: Phosphorus by Ascorbic Acid*, 1992; Murphy and Riley, 1962) (MDL = 1.2 μg P L^{-1}). DOC was determined using a Shimadzu TOC-LCPH/CPN analyzer (Shimadzu) following HCl addition (< pH 2) to degas dissolved inorganic carbon (DIC) (MDL 71 μg C L^{-1}).

Chloride, nitrate, nitrite and sulfate concentrations were measured by ion chromatography using a Dionex ICS 5000 equipped with a capillary IonPac® AS18 column. Aqueous sulfide was stabilized with 20 μL 1% zinc acetate per mL (Pomeroy, 1954) after filtering and determined by the Cline method (Cline, 1969) (MDL 0.5 µM). $Fe^{2+}_{(aq)}$ was determined by the ferrozine method immediately after filtering (Stookey, 1970; Viollier et al., 2000) (MDL 3.8 μM). All aqueous analyses were conducted in triplicate. The precision and accuracy for all techniques was < 5 RSD% and ±10% with respect to certified reference materials (where commercially available).

Solid phase methods: Phosphorus and Iron Speciation

Phosphorus partitioning within the solid phase in the reactor experiment was evaluated over a time series by both sequential extractions, using a modification (Baldwin, 1996) of the SEDEX extraction scheme (Ruttenberg, 1992) and solution ^{31}P NMR spectroscopy (Cade-Menun, 2005).

Chris Parsons 2017-4-30 11:08
Deleted: . All reagents

Chris Parsons 2017-4-30 11:08
Deleted: TDP (

Chris Parsons 2017-4-30 11:08
Deleted:)

Chris Parsons 2017-4-25 13:11
Deleted: Method detection limit

Chris Parsons 2017-5-5 10:37
Deleted: s

Chris Parsons 2017-4-25 13:29
Deleted: Method detection limit (

Chris Parsons 2017-4-30 11:09
Deleted:)

Chris Parsons 2017-4-30 11:09
Deleted:)

Chris Parsons 2017-5-4 11:37
Deleted: s

Chris Parsons 2017-5-5 10:38
Deleted: the

Chris Parsons 2017-4-30 03:57
Deleted: Fe^{2+} generated by dissimilatory iron reduction has been shown to sorb to mineral surfaces in sediment (Gehin et al., 2007; Klein et al., 2010; Liger et al., 1999) or precipitate as ferrous carbonate (Jensen et al., 2002), ferrous sulfide or other mixed ferrous/ferric phases (Rickard and Morse, 2005). Total Fe^{2+} production during anoxic half-cycles was estimated by a partial extraction (1 hour, 0.5N HCl) on sampled suspensions. Fe^{2+}/Fe^{3+} ratios were determined in extracts using a modification of the ferrozine method (Stookey, 1970; Viollier et al., 2000).

Chris Parsons 2017-4-30 17:51
Deleted: by

The two approaches are complementary; ^{31}P NMR spectroscopy provides information on the molecular speciation of phosphorus, while sequential extraction provides information on the association of the P species with operationally defined solid phase fractions. Therefore the combination of these two methods reveals redistribution of P within the solid phase over time during oxic-anoxic transitions.

The original SEDEX extraction scheme quantifies five different P reservoirs within sediment by consecutively solubilizing progressively more recalcitrant phases by using extracts of increasing severity. The reaction mechanisms associated with each extraction step are discussed in detail within Ruttenberg (1992). A modification of the SEDEX extraction scheme proposed by Baldwin (1996), used here, incorporates an additional 16 hour, 1M $NaHCO_3$ step (P_{Hum}) after the P_{Ex} step, to differentiate OM associated P which may otherwise be co-extracted during the P_{Fe} step. The pH of the $NaHCO_3$ extraction step was adjusted to 7.6 to minimize dissolution of carbonates prior to the P_{CFA} extraction step. A total of 15 samples between day 11 and 74 of the reactor experiment were analyzed in duplicate by sequential extraction. A summary of the full sequential extraction method used, including target phases, reactants, pH, temperature and reaction times is provided in Table 1.

Changes to iron speciation were also evaluated through a time series during the experiment. To account for surface-sorbed or freshly precipitated Fe, total Fe^{2+} production during anoxic half-cycles was estimated by a partial extraction (1 hour, 0.5N HCl) on sampled suspensions. Fe^{2+}/Fe^{3+} ratios were determined in extracts using a modification of the ferrozine method (Stookey, 1970; Viollier et al., 2000). Additionally, a thermodynamic model was implemented in PHREEQC (Parkhurst et al., 1999) to assess the saturation index (SI) of various minerals over time during the reactor experiment using measured pH, temperature, E_h and concentration data.

Chris Parsons 2017-5-5 10:39
Deleted: level

Chris Parsons 2017-5-3 13:42
Deleted: .

Chris Parsons 2017-4-30 03:51
Deleted: The modification of the

Chris Parsons 2017-4-30 02:41
Deleted:

Chris Parsons 2017-5-3 13:24
Deleted: adds

Chris Parsons 2017-5-3 13:24
Deleted: a

Chris Parsons 2017-4-29 17:33
Formatted: Subscript

Unknown
Field Code Changed

Chris Parsons 2017-4-30 11:15
Deleted: (Baldwin, 1996)

Chris Parsons 2017-4-30 02:41
Deleted: ,

Chris Parsons 2017-4-29 17:29
Formatted: Subscript

Chris Parsons 2017-4-29 17:22
Deleted: step to differentiate between P associated with

Chris Parsons 2017-4-29 17:27
Formatted: Subscript

Chris Parsons 2017-4-30 19:47
Formatted: Subscript

Chris Parsons 2017-4-29 17:27
Deleted: metal-OM bridging complexes and truly reducible oxide associated P. Without this modification Li et (Li et al., 2015) al have shown that CDB also extracts fine oxide-OM-P complexes. The final extraction scheme distinguishes the following fractions: Easily exchangeable (P_{Ex}, 1M $MgCl_2$), humic-bound (P_{Hum} 1M $NaHCO_3$), oxide bound (P_{Fe}, CDB), $CaCO_3$ bound (P_{CFA}, 1M Acetate pH 4), detrital apatite/other inorganic P (P_{Detr}, 1M HCl), organic-P (P_{Resi}, 1M HCl after ashing at 550 °C).

NaOH-EDTA Extraction and Solution ^{31}P NMR Spectroscopy

Molecular changes to P speciation were evaluated over a time series by solution ^{31}P NMR. Phosphorus was extracted directly from suspension samples (~2 g dry weight equivalent) prior to ^{31}P NMR analysis. The method used has been shown to allow quantitative analyses of P_o (monoester and diester), polyphosphates and orthophosphate (Amirbahman et al., 2013; Cade-Menun et al., 2006, p.; Cade-Menun and Preston, 1996; Reitzel et al., 2007; Turner et al., 2003b). Briefly, Samples were extracted in 25 mL of 0.25 M (NaOH) and Na_2EDTA (0.05 M) at ambient laboratory temperature (~22 ^{o}C) for 4 hours. Subsequently, the tubes were centrifuged (3500 rpm for 20 minutes), the supernatant extracted via syringe then neutralized with 2M HCl to a pH of 7 to avoid the breakdown of polyphosphates during freeze drying (Cade-Menun et al., 2006). This solution was then filtered to < 0.45 µm. Prior to freeze-drying 1 mL aliquots of each sample were diluted and analyzed by ICP-OES spectroscopy for Al, Ca, Fe, Mg, Mn and P. The remaining extracts were frozen at -80 ^{o}C and lyophilized for 48 hours. The lyophilized extracts were re-dissolved in 1.0 ml D_2O, 0.6 ml 10 M NaOH, and 0.6 ml of the NaOH-EDTA extractant solution and were allowed to stand for 10 min with occasional vortexing. Samples were centrifuged for 20 min at 3500 rpm, transferred to 10-mm NMR tubes, and stored at 4 °C before analysis within 12 hours.

Solution ^{31}P NMR spectra were obtained using a 600-MHz spectrometer equipped with a 10-mm broadband probe. The NMR parameters were: 90° pulse, 0.68-s acquisition time, 4.32-s pulse delay, 12 Hz spinning, 20 °C, 2200 to 2900 scans (3-4h) for 0-5cm sediment samples (Cade-Menun et al., 2010). Phosphorus compounds were identified by their chemical shifts related to an external orthophosphoric acid standard, with the orthophosphate peak in all spectra standardized to 6ppm. Peak areas were calculated by integration on spectra processed with 10 and 7-Hz line

Chris Parsons 2017-4-30 04:05
Deleted: solution

Chris Parsons 2017-4-30 04:06
Deleted: (Cade-Menun and Preston, 1996)

Unknown
Field Code Changed

Chris Parsons 2017-4-30 04:07
Deleted: (Amirbahman et al., 2013; Cade-Menun et al., 2006, p.; Reitzel et al., 2007; Turner et al., 2003)

Chris Parsons 2017-5-5 10:44
Deleted: and

Chris Parsons 2017-5-5 10:45
Deleted: to

Chris Parsons 2017-4-30 11:23
Deleted:

Chris Parsons 2017-5-4 11:39
Deleted: supernatant

Chris Parsons 2017-5-4 11:42
Deleted: s

broadening, using NUTS software (Acorn NMR, Livermore CA, 2000 edition). Peak assignments were grouped into compounds or groups of specific compound classes if direct identifications could not be made (Cade-Menun, 2005).

Extracellular enzyme assays

Rates of enzymatic hydrolysis of P_o were estimated through extracellular enzyme activities (EEA). Degradation rates for phosphomonoesters, phosphodiesters and pyrophosphate were determined fluorometrically through use of the MUF tagged substrates; MUF phosphate (MUP), Bis(MUF)phosphate (DiMUP, Chem-Impex International), and MUF pyrophosphate, (PYRO-P), Chem-Impex International) respectively. Additionally MUF β-D-glucopyranoside (MUGb) was used in order to compare phosphatase enzyme activity to the activity of β-glucosidase (cellulase) (Dunn et al., 2013). Enzyme activities were determined using a microplate reader (Flexstation3, Molecular Devices) using a modification of Deng et al (2013). Briefly, 1 g dry weight equivalent of suspension from the reactor was stirred with 100 mL of 100 mM HEPES buffer at pH 7.5 in a pyrex dish for 10 minutes at 280 rpm to allow for complete homogenization. Subsamples (100 µL) of the buffered soil suspension were removed during continuous mixing using a multi-channel pipette and placed into microplate wells, which were loaded into the microplate reader. Four replicate wells were filled per substrate. Plates were left to equilibrate at 30 °C for 5 minutes inside the reader before the automatic addition of 100 µL of substrate, resulting in a final substrate concentration of 667 µM. Each well was triturated thoroughly during addition of the substrate. Excitation fluorescence was set at 365 nm. Emission intensity at 450 nm was recorded at 5-minute intervals over a 6-hour period. The effect of fluorescence quenching was accounted for in each sample by preparing MUF calibration curves in the same soil suspension as used for the analysis. The limits of detection and quantification were

Unknown
Field Code Changed

Chris Parsons 2017-5-5 10:47
Deleted: (Deng et al., 2013)

Chris Parsons 2017-4-26 16:36
Deleted: wa

Chris Parsons 2017-4-26 16:36
Deleted: s subsequently recorded 6 times at

Chris Parsons 2017-4-26 16:36
Deleted:

Chris Parsons 2017-4-26 16:37
Deleted: 5 minute

Chris Parsons 2017-4-30 11:24
Deleted:

Chris Parsons 2017-4-30 11:24
Deleted: as

determined to be 1.1 µM and 3.3 µM MUF respectively, equivalent to 1.1 µM of phosphate for the determination of phosphomonoesterase activities.

RESULTS & DISCUSSION

Sediment characterisation and evidence of bioturbation

Characterisation of sediment cores revealed physical and chemical solid phase homogeneity within the top 10 cm, with a bulk density of ~1.3 g cm^{-3}, water content of ~50% (by weight), OM of ~3% and a carbonate of ~25% (Figure 2B). Between 10 and 15 cm depth increases in bulk density and decreases to the sediment water content, OM % and carbonate fraction occurred as soft sediment transitioned to clay.

A benthic macroinvertebrate density of approximately 49,500 individuals per m^2 was determined, consistent with previously reported values (Pelegri and Blackburn, 1995). The community (Figure 2A) was dominated by aquatic earthworms (*Tubificidae 60%* and *Branchiura sowerbyii 8%*) which typically feed and mix sediment within the top 5-10 cm (Fisher et al., 1980; McCall and Fisher, 1980). Other groups identified included *Ceratopogonidae* (No see ums or biting midges, 22%) including *Sphareomias*, *Probezzia* and *Bezzia, Chironomidae* (Midges, 6%) including *Cryptochironomus* and *Tanypus, Nemotoda* (round worms, 4%) and a single *Hyalella azteca* (scud <1%).

Bioturbating organisms, such as those identified, have previously been shown to alter biogeochemical cycling within surface sediments (Hölker et al., 2015). Reported influences include increased solute fluxes (Furukawa et al., 2001; Matisoff and Wang, 1998), mixing of solid sediment (Fisher et al., 1980) and bioconveying of sediment particles (Lagauzère et al.,

Chris Parsons 2017-4-30 11:24
Deleted: MUF and the limit of quantification to be

Chris Parsons 2017-4-30 11:24
Deleted: (

Chris Parsons 2017-4-30 11:24
Deleted:)

Chris Parsons 2017-5-3 12:11
Deleted: ... [4]

Chris Parsons 2017-4-30 03:10
Deleted: 0-

Chris Parsons 2017-4-30 03:10
Deleted: occur

Chris Parsons 2017-4-30 03:10
Deleted: transitions

Chris Parsons 2017-4-30 11:26
Deleted: B

Chris Parsons 2017-4-30 11:26
Deleted: is

Chris Parsons 2017-4-30 11:26
Deleted: densities of 50,000 individuals per m^2

Chris Parsons 2017-4-30 03:11
Deleted: composition is shown in Figure 2A. The community

Chris Parsons 2017-5-5 10:48
Deleted: which were not further identified,

Chris Parsons 2017-4-30 11:27
Deleted: by

Chris Parsons 2017-4-30 11:28
Deleted: ing

Chris Parsons 2017-4-30 11:28
Deleted: increasing

2009). These processes have been shown to enhance sediment oxygen demand (McCall and Fisher, 1980; Pelegri and Blackburn, 1995), degradation of OM (Aller, 1994), rates of denitrification, transport of contaminants to surface water (Lagauzère et al., 2009), and temporal fluctuation of redox conditions (Aller, 1994). Efficient sediment mixing allows frequent re-oxidation of reduced sediments and therefore regeneration of terminal electron acceptors (TEAs) such as nitrate, ferric iron and sulfate, which often limit mineralisation of OM in sediments underlying hypereutrophic water bodies (Reddy and DeLaune, 2008). Electron donors in the form of fresh autochthonous necromass are also rapidly redistributed vertically within the zone of bioturbation. This environment should therefore support a metabolically diverse, abundant and highly active microbial community (DeAngelis et al., 2010).

Quantitative XRD analysis of the top 12 cm of sediment (Figure 2C) showed close agreement with the carbonate fraction determined by TGA (~25% by TGA vs 27% by XRD) indicating a calcite dominated, carbonate buffered system. The remaining mineral assemblage was dominated by quartz and clay minerals (Illite, 30% and Chamosite, 2%). No pyrite or vivianite was detected by XRD suggesting either their absence or presence in low abundance (<1%) with poorly crystalline structures.

Experimental redox oscillation: Aqueous chemistry

E_h within the bioreactor oscillated between +470 and -250 mV (Figure 3) consistent with E_h ranges of wetland sediments (Nikolausz et al., 2008). A slight pH oscillation was also present between ~7.4 during anoxic half-cycles (N_2 sparging) and ~7.7 during oxic-half cycles (N_2:O_2:CO_2 sparging), this variation, shown in Figure 3, is consistent with calcite/dolomite buffered sediment equilibrating with changing p_{CO2} caused by sparging gas composition and microbial respiration. After the 11-day equilibration, ionic strength of the aqueous phase in the

Chris Parsons 2017-4-30 02:44
Deleted: enhance

Chris Parsons 2017-4-30 03:12
Deleted: increase

Chris Parsons 2017-4-30 03:12
Deleted: increase

Chris Parsons 2017-4-30 03:12
Deleted: increase

Chris Parsons 2017-4-30 03:13
Deleted: (Furukawa et al., 2001)

Chris Parsons 2017-4-30 03:13
Deleted:

Chris Parsons 2017-5-3 13:00
Deleted:

Chris Parsons 2017-4-30 11:41
Deleted: In contrast

Chris Parsons 2017-4-30 11:41
Deleted: ,

Chris Parsons 2017-4-30 11:41
Deleted: conditions

Chris Parsons 2017-4-30 11:41
Deleted: within the sediment suspension remained constant between 7.2 and 7.5 for the duration of the experimen

Chris Parsons 2017-4-30 14:40
Formatted: Subscript

Chris Parsons 2017-4-30 11:41
Deleted: t

Chris Parsons 2017-4-30 14:40
Formatted: Subscript

Chris Parsons 2017-4-30 14:40
Formatted: Subscript

Chris Parsons 2017-4-30 14:40
Formatted: Subscript

Chris Parsons 2017-4-30 03:15
Deleted: , as identified via XRD analyses

Chris Parsons 2017-4-30 11:46
Deleted: ,

Chris Parsons 2017-4-30 11:46
Deleted: at

Chris Parsons 2017-4-30 11:48
Deleted: of ~$10^{-1.8}$ atm

reactor suspension remained at ~0.025 +/- 0.004 M for the duration of the experiment. This range of E_h/pH conditions and ionic strength is consistent with the range measured within surficial sediment at the field site and transitions across the thermodynamically predicted stability boundaries for multiple redox couples e.g. MnO_2/Mn^{2+}, $NO_3^-/NO_2^-/NH_4^+$, $Fe(OH)_3/Fe^{2+}$, SO_4^{2-}/HS^- during each 14 day redox cycle. The upper E_h values recorded during oxic cycles are significantly lower than predicted by the O_2/H_2O couple (820 mV @ pH 7) but are consistent with the O_2/H_2O_2 couple (300 mV @ pH 7) which is considered to control electrode measured E_h under oxic conditions (Stumm and Morgan, 1996).

Aqueous chemistry data, shown in Figure 3, demonstrate the consumption of TEAs in order of decreasing nominal energetic yield, coupled to the oxidation of labile OM. Upon physical removal and consumption of residual oxygen by aerobic respiration, nitrate concentration decreased in the solution. Decreases to nitrate concentration coincided with peaks of nitrite concentration within the first hour of oxygen removal, indicative of microbial denitrification. Subsequent increases to $Mn_{(aq)}$, $Fe^{2+}_{(aq)}$ and $HS^-_{(aq)}$ imply sequential reduction of MnO_2, $Fe(OH)_3$ and SO_4^{2-} as more energetically efficient electron acceptors were depleted. Mn (predicted as Mn^{2+} by the thermodynamic model) and Fe^{2+} were detected in solution earlier within each subsequent anoxic cycle, however the apparent order of reduction remained consistent across all five redox cycles (O_2, NO_3^-, NO_2^-, MnO_2, $Fe(OH)_3$, SO_4^{2-}). The consistent order and relative magnitude of reduction implies that the main biogeochemical functioning of the sediment suspension did not change dramatically between cycles during the experiment.

Although relatively low concentrations of Fe^{2+} (up to 71 μM) were measured in solution, 0.5 M HCl extractions revealed that significantly greater Fe^{2+} was produced during each anoxic cycle than was measured in the aqueous phase. Fe^{2+} generated by dissimilatory iron reduction has been

Chris Parsons 2017-5-3 13:02
Deleted: implies

Chris Parsons 2017-5-3 12:24
Deleted: OOH

Chris Parsons 2017-5-3 12:24
Formatted: Subscript

Chris Parsons 2017-5-5 10:52
Formatted: Not Superscript/ Subscript

Chris Parsons 2017-5-5 10:51
Deleted: ,

Chris Parsons 2017-5-3 13:02
Deleted: the…aerobic respiration, nitrate ... [5]

Chris Parsons 2017-5-3 12:24
Deleted: OOH…and …O_4^{2-} as more energ ... [6]

Chris Parsons 2017-5-3 12:24
Formatted: Subscript

Chris Parsons 2017-5-3 12:25
Formatted: Subscript

Chris Parsons 2017-4-30 03:25
Deleted: Relatively …lthough relatively lo ... [7]

shown to sorb to mineral surfaces in sediment (Gehin et al., 2007; Klein et al., 2010; Liger et al., 1999) or precipitate as ferrous carbonate (Jensen et al., 2002), ferrous sulfide or other mixed ferrous/ferric phases (Rickard and Morse, 2005). The 0.5M HCl extractions targeted this sorbed or poorly crystalline freshly precipitated Fe^{2+}. During each anoxic cycle HCl extractable Fe^{2+} concentration increased by 50 to 70 μmol g^{-1}, equivalent to 12.31 to 17.29 mM of iron reduction within the reactor as a whole. Thus, only 0.63 +/- 0.4% of microbially reduced Fe^{2+} was measureable in solution. The aqueous phase of the reactor was shown to be supersaturated with respect to mackinawite (FeS), pyrite (FeS_2), vivianite ($Fe_3(PO_4)_2{:}8H_2O$) and siderite ($FeCO_3$) during anoxic half-cycles indicating thermodynamic favourability for precipitation of these minerals. The kinetic constraints on precipitation were not, however, considered. No significant cumulative change to extractable Fe^{2+}/Fe^{3+} occurred after five full reduction-oxidation cycles, indicating that solid phase Fe redox cycling was reversible, potentially due to rapid oxidation of solid Fe^{2+} in the presence of O_2 and carbonate (Caldeira et al., 2010).

DOC concentration also fluctuated systematically during oxic-anoxic cycles (Figure 3). Higher DOC concentrations were measured during anoxic conditions than oxic conditions. DOC may be replenished by both enzymatic hydrolysis of particulate organic matter (POM) (Vetter et al., 1998) and desorption of mineral associated OM (Grybos et al., 2009). The addition of algal matter at the beginning of anoxic cycles resulted in observable sharp peaks of DOC which was rapidly removed from solution, probably due to a combination of mineralization of labile DOC to HCO_3^- and sorption processes (Chorover and Amistadi, 2001; Grybos et al., 2009). The peak of DOC supplied by addition of algal matter represented labile DOC, which was readily mineralized in comparison to the residual DOC, which persisted in the system throughout the experiment. The differences in residual OM mobility between oxic and anoxic cycles were

Chris Parsons 2017-4-30 03:26
Deleted: Within the 0.5M HCl extractable solid phase, changes to …xtractable Fe^{2+} concentra... [8]

Chris Parsons 2017-4-30 17:31
Formatted: Superscript

Chris Parsons 2017-5-3 13:07
Formatted ... [9]

Chris Parsons 2017-4-30 03:32
Deleted: Although iron reduction varied between 50 and 70 μmol g^{-1} between cycles, the relative proportion of $Fe^{2+}_{(aq)}$ remained low at 0.63 +... [10]

Chris Parsons 2017-4-30 03:37
Deleted: s…also , shown in Figure 3, …lu... [11]

unlikely due to oxide dissolution as differences to DOC concentration are observed prior to increases in Mn and Fe concentration in solution. We therefore postulate that solubility changes to humified DOC were driven by pH changes (Figure 3) between oxic and anoxic conditions caused by changes in pCO_2 between oxic and anoxic conditions as previously shown by Grybos et al in wetland sediments (Grybos et al., 2009).

Lowest aqueous phosphorus concentrations (~2.5 to 3 μM), shown in Figure 4, occurred during oxic half cycles and increased dramatically during anoxic half cycles to a maximum concentration of 50 to 60 μM per cycle, 88% of which occurred as SRP. The range of TDP concentrations within the aqueous phase of the reactor suspension are similar to those reported in situ at the field site by Mayer et al (2006). The timing of phosphorus release to the aqueous phase corresponded well with increasing $Fe^{2+}_{(aq)}$ concentration. This is reflected in a strong positive correlation between TDP and Fe concentrations ($n = 37$, $R^2 = 0.93$, $p < 0.0001$). Increases to aqueous P concentration occurred only after depletion of residual O_2, NO_3^- and NO_2^-, after increases to $Mn_{(aq)}$ and before increases to $HS^-_{(aq)}$. The timing of P release is suggestive of an iron(III)-oxyhydroxide or ferric phosphate control on phosphorus mobility (Bonneville et al., 2004; Hyacinthe and Van Cappellen, 2004) and indicates that complete nitrate depletion was required prior to phosphorus release to the aqueous phase. Full tabulated aqueous chemistry data for the experimental time series is provided as supporting information.

Sequential chemical extractions and solid phase P partitioning

The sum of P concentrations from all sequential extraction reservoirs (61 ± 5 μmol g^{-1}) was consistently within 10% of a total P extraction (57 ± 4 μmol g^{-1}) indicating acceptable analytical precision from the sequential extraction procedure. Highest P concentrations were associated with the P_{Hum} (~26% of TP) and P_{Fe} (~24%) fractions with lower P concentrations in the P_{Ex}

Chris Parsons 2017-4-30 03:39
Deleted: to be …ue to oxide dissolution a... [12]

Chris Parsons 2017-4-30 03:42
Deleted: (~2.5 to 3 μM)

Chris Parsons 2017-4-30 03:42
Deleted: (Mayer et al., 2006).… The timi... [13]

Unknown
Field Code Changed

Chris Parsons 2017-4-29 18:12
Moved down [3]: Sequential extractions provide further evidence for a ferric (hydr)oxide control on aqueous P concentrations (Figure 4).

Chris Parsons 2017-4-30 11:58
Deleted: s…(61 ± 5 μmol g^{-1}) was consist... [14]

~16%, P_{CFA} ~15%, P_{Detr} ~12% and P_{Res} ~7% fractions (Figure 4). The largest variations in P concentration were observed for P_{Fe} and decreased in the order P_{Fe} (2.6) > P_{Hum} (1.5) > P_{Ex} (0.4) > P_{Detr} (0.4) > P_{Resi} (0.35) > P_{CFA} (0.25), where the numbers in brackets are standard deviations (μmol g^{-1}). High variability over time within the P_{Fe} and P_{Hum} fractions suggests that P was exchanged to and from these fractions during redox oscillation whereas changes to the P_{Ex}, P_{Resi} and P_{CFA} fractions were comparatively insignificant (Figure 4).

The P_{Fe} fraction was the only P pool in which concentration consistently decreased during anoxic conditions and increased during oxic conditions (Figure 4). When a P mass balance (Figure 5) was attempted to account for increases to aqueous phosphorus (P_{Aq}) from the iron bound (P_{Fe}) pool during anoxic periods it became evident that only approximately 4.5% of variability observed in the P_{Fe} pool (total P_{Fe} variation of up to 4.5 μmol g^{-1} during anoxic periods) was necessary to account for the changes to inter-cycle P_{Aq} concentrations (50 μM). The remainder of P_{Fe} lost during anoxic cycles appears to be reversibly redistributed to the P_{Ex} (~30%) and P_{Hum} (~65%) pools which generally increased during anoxic conditions and decreased during oxic conditions (Figure 4).

According to Ruttenberg (1992) the P_{Ex} fraction corresponds to P mobilised via the formation of $MgPO_4^-$ complexes and(or) mass action displacement by Cl^-. It is therefore considered that $MgCl_2$ effectively extracts P loosely associated with mineral surfaces. However, Ruttenberg (1992) also demonstrated that plankton were efficiently extracted by $MgCl_2$ as well as ~25% of P associated with biogenic $CaCO_3$. Consequently, it is likely that P associated with microbial biomass, $CaCO_3$, and other loosely sorbed P contributed to the P_{Ex} fraction. Slight increases to P_{Ex} concentration during anoxic periods and corresponding decreases during oxic periods likely reflect the combination of two processes 1) equilibration between P surface complexes and

Chris Parsons 2017-5-4 14:45
Formatted ... [15]

Chris Parsons 2017-4-30 01:01
Moved (insertion) [4]

Chris Parsons 2017-4-30 01:07
Deleted: Although only ~24% of TP was associated with the CDB extractable pool (P ... [16]

Chris Parsons 2017-4-29 18:18
Formatted ... [17]

aqueous P species due to fluctuating aqueous concentrations which were consistently higher during anoxic periods (Olsen and Watanabe, 1957) and 2) pH driven sorption/desorption as pH was consistently slightly higher during aerobic periods (Figure 3) favouring desorption from mineral surfaces including illite which comprised 30% of the crystalline mineralogical fraction (Figure 2C) (Manning, 1996).

The $NaHCO_3$ extraction step was originally added to the SEDEX method to target OM associated P, which would otherwise be liberated during the P_{Fe} extraction step (Baldwin, 1996). Baldwin noted a brown coloration in P_{Hum} extracts and that absorbance at 250 nm was positively correlated with SRP. Absorbance at 254 nm has been shown to be indicative of aromatic OM, commonly associated with humic substances (Weishaar et al., 2003). A light brown color was also present in the $NaHCO_3$ extracts recovered during this experiment despite comparatively low sediment OM content (Figure 2B). Absorbance spectra for these extracts were not determined.

Li et al (2015) have recently demonstrated that the SEDEX P_{Fe} extraction step co-extracted P associated with fine iron oxide-OM complexes when a prior $NaHCO_3$ step was not incorporated. However, Li et al (2015) also suggested that these complexes may be more recalcitrant than pure minerals. Iron was present within the P_{Hum} extract at concentrations between 18 and 25 μmol g^{-1} however, the original speciation of this iron is prior to extraction is unknown. Chemically similar extractions used in soil sciences such as Hedley's extraction (0.5 M $NaHCO_3$, pH 8.5, 16 hours) and the Olsen-P test (0.5M $NaHCO_3$, pH 8.5, 30 minutes) have been shown to extract Mg and Ca phosphates as well as some organic P (Hedley et al., 1982; Olsen et al., 1954). Approximately 2/3 of P extracted within P_{Hum} was present as SRP suggesting that ~1/3 of this fraction may be P_o species. The pH of the $NaHCO_3$ extract used here was adjusted to 7.6 to minimize the dissolution of Mg and Ca phosphates prior to the P_{CFA} extraction. Despite this, 30 to 44 μmol g^{-1} of Ca was

Chris Parsons 2017-5-5 11:11
Formatted: English (UK)

Chris Parsons 2017-4-30 02:55
Formatted: Normal, Line spacing: double

Chris Parsons 2017-4-29 19:46
Formatted: Subscript

Chris Parsons 2017-4-29 19:47
Formatted: Subscript

Chris Parsons 2017-4-30 00:14
Formatted: Subscript

Chris Parsons 2017-4-29 21:58
Formatted: Subscript

Chris Parsons 2017-4-29 23:29
Formatted: Subscript

Chris Parsons 2017-4-30 21:01
Formatted: Subscript

Chris Parsons 2017-4-30 19:12
Formatted: Subscript

Chris Parsons 2017-4-30 19:13
Formatted: Subscript

Chris Parsons 2017-4-30 19:20
Formatted: Subscript

Chris Parsons 2017-4-30 19:20
Formatted: Subscript

Chris Parsons 2017-4-30 20:30
Formatted: Subscript

Chris Parsons 2017-4-30 20:31
Formatted: Subscript

extracted within the P_{Hum} fraction. The origin of the extracted Ca is, however, unknown and may have been complexed with OM or part of labile Ca-phosphates. It is still expected that the majority of Ca-phosphate minerals were quantified as part of the P_{CFA} or P_{Detri} extractions which included ~500 to 700 and ~50 to 70 μmol Ca g^{-1} respectively.

Humic acids are known to compete with orthophosphate for surface binding sites on various minerals including goethite (Sibanda and Young, 1986) and poorly ordered Fe-oxides in the short term (Gerke, 1993). However, sorption of natural OM to freshly precipitated Fe oxides may increase the long term sorption capacity of ferric oxides towards P by decreasing recrystallization over time (Gerke, 1993) and through the formation of OM-Fe-P complexes (Gerke, 1993). Although previous studies have provided evidence for ternary complexes between ferric iron, OM and phosphate (Kizewski et al., 2010b) there is currently no direct spectroscopic evidence for the existence of mixed OM-Fe(III)-phosphate complexes in natural waters. Identification of such complexes in natural environments is inherently challenging due to the complexity of natural geochemical matrices (Kizewski et al., 2010a). Recent studies have however successfully investigated the structure of synthetic OM-Fe(III)-phosphate complexes (Kizewski et al., 2010a) and similar OM-Fe(III)-arsenate complexes spectroscopically (Mikutta and Kretzschmar, 2011; Sharma et al., 2010). These studies suggest that similar and perhaps more complex heterogeneous ternary complexes are also likely to be present in natural freshwater environments (Kizewski et al., 2010a). This suggestion is also supported by the observation that more than 80% of soluble P in some natural waters is associated with high molecular weight OM (Gerke, 2010). As spectroscopic characterization of the P associated with the P_{Hum} fraction was not performed in this study, the P_{Hum} pool is considered to represent a variety of OM associated P in addition to small amounts of P from labile Ca-phosphate minerals.

Chris Parsons 2017-4-30 20:46
Formatted: Subscript

Chris Parsons 2017-4-30 21:07
Formatted: Subscript

Chris Parsons 2017-4-30 21:07
Formatted: Subscript

Chris Parsons 2017-5-4 14:53
Comment [1]: Break up paragraph

OM associated P extracted within this fraction is likely coordinated with ferric iron (18 to 25 μmol Fe g^{-1} coextracted), Ca (30 to 44 μmol Ca g^{-1} coextracted) or Al (0.8 to 1.5 μmol Al g^{-1} coextracted). These metals may, in-turn, be associated with various mineral surfaces within the sediment.

Sequential extraction data demonstrate that the P_{Hum} fraction is the dominant P fraction in all samples analysed, which highlights the significance of this fraction. P mass balance also suggests that reversible re-partitioning between this and the P_{Fe} fraction occurs during redox condition changes. As the exact chemical nature of the P_{Hum} fraction is not known, interpretation of concentration changes over time are challenging. Speculatively, increases to the P_{Hum} fraction under anoxic conditions may be due to the release of occluded OM-metal-P complexes within iron(III) oxyhydroxides during reductive dissolution or simply re-equilibration of solid phase OM-metal-P complexes with increased aqueous P.

We consider that the majority of P extracted within the P_{Fe} fraction was co-precipitated with iron(III)-oxyhydroxides which were reductively dissolved by dithionite during the extraction (Ruttenberg, 1992). This interpretation is supported by the relatively high concentrations of iron extracted within the P_{Fe} fraction (72 to 91 μmol Fe g^{-1}). Aqueous Fe^{2+} produced during this extraction is subsequently chelated by citrate and therefore solubility of Fe and P is maintained. The bicarbonate component functions as a pH buffer to ensure maximum preservation of apatite and $CaCO_3$ bound P during this reaction step (Ruttenberg, 1992).

Neither the P_{CFA}, P_{Detri} nor P_{Resi} fractions varied systematically between oxic and anoxic conditions, or changed consistently during the course of the experiment, suggesting their comparative stability during short periods of redox fluctuation this is supported by calculated

Chris Parsons 2017-4-30 02:57
Formatted: Subscript

Chris Parsons 2017-4-30 01:29
Formatted: Subscript

Chris Parsons 2017-4-30 03:04
Formatted: Superscript

Chris Parsons 2017-4-30 01:39
Formatted: Subscript

Chris Parsons 2017-4-30 01:47
Formatted: Subscript

saturation indices (SI) for hydroxyapatite, which remained between +0.86 and +6.24 for the duration of the experiment.

The P contribution from individual algal additions (~1.5 μmol P g^{-1}) was relatively small compared to total P in the reactor (61 μmol P g^{-1}) and within the margin of analytical error associated with solid extractions. Additionally, no single fraction shows a clear increase over the course of the experiment, therefore quantification of the redistribution of P added with algal additions is not possible.

Full tabulated solid phase chemistry data for the experimental time series is provided as supporting information.

Fe:P ratios

Sequential extraction data, shown in Figure 4, aqueous chemistry data shown in Figure 3, and the correlation between aqueous Fe and P ($n = 37$, $R^2 = 0.93$, $p < 0.0001$) all suggest that P released to solution under anoxic conditions originated in the P_{Fe} pool. Although the maximum molar ratio for phosphate incorporation within ferric oxides has been shown to be 2:1 (Fe:P) (Thibault et al., 2009), it has been suggested that much higher solid Fe:P of 15 (Jensen et al., 1992) to >20 (Phillips et al., 1994) maybe necessary to control phosphorus mobility under oxic conditions. Results from bioreactor experiments suggest that phosphorus is retained in the solid phase under oxic conditions at total Fe:P ratios of just 4.1:1, potentially due to the association of P with other solid sedimentary pools, particularly P_{Hum}. Fe:P ratios below the stoichiometric limitation of 2:1, measured in the aqueous phase (1.5 to 1.9), during anoxic conditions are therefore likely due to the removal of Fe^{2+} from solution by secondary sorption and precipitation processes, subsequent to reductive dissolution. Probable secondary Fe^{2+} removal processes include the formation of amorphous FeS (SI of up to +2.27 for mackinawite) (Rickard and Morse, 2005) and sorption of

Chris Parsons 2017-4-29 18:12
Moved (insertion) [3]

Chris Parsons 2017-4-30 01:01
Moved up [4]: Although only ~24% of TP was associated with the CDB extractable pool (P_{Fe}). The P_{Fe} fraction shows greater inter-cycle variability than other solid phase P pools and is the only P pool in which concentration consistently decreased during anoxic conditions and increased during oxic conditions. Notably the calcium bound (P_{CFA}) pool exhibited no P im/mobilization behaviour due to changes in redox conditions. When a P mass balance (Figure 5) is attempted to account for increases to aqueous phosphorus (P_{Aq}) from the iron bound (P_{Fe}) pool during anoxic periods it becomes evident that only approximately 4.5% of variability observed in the P_{Fe} pool (total P_{Fe} variation of up to 4.5 μmol g^{-1} during anoxic periods) is necessary to account for the changes to inter-cycle P_{Aq} concentrations (50 μM). The remainder of the P_{Fe} lost during anoxic cycles appears to be reversibly redistributed to the P_{Ex} (~30%) and P_{Hum} (~65%) pools. The lack of significant P_{Resi} (~7%) despite consistently high primary productivity in the sampling location may suggest that P_o additions are rapidly degraded and do not accumulate annually. However, it has been shown that P from fresh algal biomass may be released during the first extraction step of the SEDEX protocol (P_{Ex}) (Ruttenberg, 1992), this fraction is also relatively minor compared to total P concentrations (~16%). The P contribution from individual algal additions (~1.5 μmol P g^{-1}) was relatively small compared to the total P mass in the reactor (61 μmol P g^{-1}) and within the margin of analytical error associated with solid extractions. Additionally, no single fraction shows a clear increase over the course of the experiment, therefore quantification of the redistribution of added P is not possible.

Chris Parsons 2017-4-26 17:02
Moved (insertion) [2]

Chris Parsons 2017-4-30 00:24
Deleted: Sequential extractions provide further evidence for a ferric (hydr)oxide control on aqueous P concentrations (Figure 4).

Chris Parsons 2017-4-29 19:59
Deleted: P associated with OM (P_{Hum}) ... [18]

Chris Parsons 2017-4-30 12:28
Deleted: phosphorus

Chris Parsons 2017-5-5 11:17
Deleted: likely

Fe^{2+} to clays (Gehin et al., 2007; Klein et al., 2010). This is supported by increases to Fe^{2+}/Fe^{3+} ratios in the 0.5 M HCl extractable fraction during anoxic conditions. Frequent rapid reoxidation of ferrous sulfide due to air sparging in the reactor experiment, and extensive bioturbation in-situ, likely prevents formation of more recalcitrant and slow forming iron sulfide minerals such as pyrite, despite strong thermodynamic favourability for pyrite formation (SI up to +13.13) (Caldeira et al., 2010; Peiffer et al., 2015). This is consistent with the results of XRD analysis, which did not identify pyrite (Figure 2C). A similar effect has been previously demonstrated in lake sediments (Gächter and Müller, 2003).

Hydrolytic enzyme activities

The activities of model phosphomonoesterases, phosphodiesterases and pyrophosphatase were found to be systematically higher under oxic conditions compared to anoxic conditions by 37% ($p < 0.005$), 8% (not significant) and 24% ($p = 0.08$) respectively (Figure 6B). Phosphomonoesterases were found to have the highest activities despite the inherent overestimation of phosphodiesterase activities when using MUF tagged substrates (Sirová et al., 2013). The opposite trend was observed for glycopyranoside, part of the cellulose degradation pathway (Dunn et al., 2013), which showed consistently higher activity (69% $p = <0.05$) under anoxic conditions (Figure 6B). The different trends exhibited by cellulose and phosphatase enzymes, indicate that changes in activity were not universal but specific to enzyme function. Phosphomonoesterase activities obtained in the current study (1.76 to 2.4 mmol h^{-1} kg^{-1}) are similar to those previously reported in wetland sediments (Kang and Freeman, 1999) and suggest the capacity for rapid hydrolysis of P_o species in necromass. Lowering of the water table in wetlands has previously been shown to increase the activity of phosphatase enzymes and the hydrolysis of P_o species (Song et al., 2007). However, water table fluctuation results in

Chris Parsons 2017-5-3 12:34
Deleted: Although considerable fresh precipitation of FeS is likely to have occurred during anoxic conditions,

Chris Parsons 2017-4-26 16:42
Deleted: due to f

Chris Parsons 2017-4-26 16:47
Deleted: permanent Fe removal in this system

Chris Parsons 2017-4-26 16:49
Deleted: as has been demonstrated previously

Chris Parsons 2017-4-30 01:45
Deleted:

Chris Parsons 2017-4-26 17:02
Moved up [2]: P associated with OM (P_{Hum})

Chris Parsons 2017-4-30 01:45
Deleted:)

Chris Parsons 2017-4-30 03:07
Deleted: s

Chris Parsons 2017-4-30 12:39
Formatted: Subscript

Chris Parsons 2017-4-30 12:39
Deleted: however, direct rate comparisons cannot be made due to different analysis conditions and the use of sediment suspensions in the current study

Chris Parsons 2017-4-30 12:40
Deleted:

concomitant changes to moisture content and redox conditions which prevents isolation of the causal variable in field investigations (Rezanezhad et al., 2014). Therefore, this is to the best of our knowledge, the first direct demonstration of phosphatase activity changes in response to changing redox conditions. We postulate that under anoxic conditions when phosphorus availability in the aqueous phase is high, production of extracellular phosphatase enzymes by the microbial community is down regulated. Conversely, when bioavailable phosphorus is removed from solution under oxic conditions, extracellular phosphatase production is up regulated in response. Adjustments to enzyme production in response to changes in phosphate availability must occur on short timescales (hours/days) for such trends to be observable during the bioreactor experiment. An inverse relationship between phosphatase activities and phosphate concentration, has previously been shown spatially in wetlands by Kang and Freeman (1999) but to our knowledge never temporally in sediments.

Chris Parsons 2017-4-26 19:55
Deleted: and changes to

Chris Parsons 2017-4-26 19:55
Deleted: simultaneously

Chris Parsons 2017-4-26 19:55
Deleted: ing

Chris Parsons 2017-4-30 12:44
Deleted: down-regulated

Chris Parsons 2017-4-30 12:43
Deleted: Alternatively

Chris Parsons 2017-4-30 12:43
Deleted: up-regulated

Chris Parsons 2017-4-30 12:44
Deleted: (Kang and Freeman, 1999)

Unknown
Field Code Changed

^{31}P NMR

Results from ^{31}P NMR analyses (Figure 6A) show that the majority of phosphorus was present in the solid phase as ortho-phosphate (84-91%) with 4-8% monoester P, 3-8% diester P and <1% phosphonates and polyphosphates with no clear trend in relative abundance emerging during the experiment. The NaOH-EDTA extraction resulted in a recovery of ~27% of TP, which is comparable to previous studies with carbonate buffered soils and sediments (Hansen et al., 2004; Turner et al., 2003a). Alpha and beta glycerophosphates are commonly identified in monoester spectral regions and have been demonstrated to be products of diesters degraded during analysis (Doolette et al., 2009; Jørgensen et al., 2015; Paraskova et al., 2015). As no glycerophosphates were identified in any of the analysed samples, recalculation of monoester/diester ratios was not performed. A higher mean monoester/diester ratio (2.31) was found in reduced samples than

Chris Parsons 2017-4-30 02:01
Deleted: despite algal additions

Chris Parsons 2017-4-29 16:14
Deleted: Therefore P_o did not represent a significant sink of P in the sampled sediment or as a result of experimental conditions

Chris Parsons 2017-4-29 16:14
Deleted: .

Chris Parsons 2017-4-30 22:59
Deleted:

oxidised samples (0.97) a statistically significant difference (p=0.04). This difference could indicate that monoester P was either less efficiently extracted under oxic conditions due to sorption to metal oxides or that monoesterase/diesterase activity decreased under anoxic conditions, which is consistent with enzymatic activity assays (Figure 6B). Total P_o determined by ^{31}P NMR varied between 9 and 16% over time compared to 5 to 11% in the P_{resi} from sequential extractions, indicating that not all P_o was extracted in the P_{resi} fraction, which is commonly referred to as the organic-P fraction. We postulate that the remaining ~5% of total phosphorus, identified as P_o by ^{31}P NMR was extracted during previous steps in the sequential extraction scheme, particularly $MgCl_2$, which has been shown to efficiently extract P associated with microbial biomass (Ruttenberg, 1992) and $NaHCO_3$. The relative activities of phosphatase enzymes appear to correlate with the relative abundances of P_o species identified by ^{31}P NMR e.g. Monoesters > Diesters > Pyro-P.

Significant polyphosphate (> 1%) was not detected by ^{31}P NMR during experiments. Previous studies focusing on WWTP tertiary treatment for phosphate removal suggest that redox oscillating conditions promote intracellular poly-P accumulation during aerobic conditions to be used as an energy store under anoxic conditions in order to uptake short chain fatty acids (SCFA) in the absence of an electron acceptor (Hupfer et al., 2007; Wentzel et al., 1991). Phosphate uptake during aerobic conditions therefore requires P availability in excess of what is required for growth and maintenance of the microbial community. However, phosphate availability under aerobic conditions is limited by sorption and coprecipitation with iron oxides, assuming sufficient Fe:P, despite high total phosphorus concentration in sediment. The P requirements by the microbial community are also likely to be high during the transition to aerobic conditions due to the availability of O_2 as an energetically efficient electron acceptor and fermentation products

Chris Parsons 2017-4-30 12:45
Deleted: P_o

Chris Parsons 2017-4-30 02:03
Formatted: Subscript

Chris Parsons 2017-5-5 11:24
Formatted: Subscript

Chris Parsons 2017-5-5 11:25
Deleted: .

(SCFA), further decreasing the probability of polyphosphate accumulation. Additionally, polyphosphate accumulation and release has shown to be inhibited by denitrification and sulfate reduction due to competition for SCFA (Kortstee et al., 1994; Yamamoto-Ikemoto et al., 1994).

IMPLICATIONS

Our controlled laboratory simulation of highly dynamic redox conditions in eutrophic sediment demonstrates the importance of multiple coupled elemental cycles (C, N, Fe, S, P) when determining internal P loading potential and timing. Our results demonstrate that neither aqueous or solid phase Fe:P ratios or even solid phase P_{Fe} quantification are good predictors of potential P release to the water column under anoxic conditions, due to extensive reversible redistribution of both reduced Fe and associated P within the solid phase. We show that 99.4% of reduced Fe and 95.5% of P_{Fe} are not released to the aqueous phase upon Fe reduction but reversibly redistributed within the solid phase upon short periods of iron reduction. Additionally, the apparent requirement for complete nitrate depletion prior to anoxia-promoted P release to the aqueous phase has potential implications for water bodies where significant iron bound legacy P is present within sediments. Our results suggest that decreasing NO_3^- concentrations in external loads, while ostensibly ecologically beneficial, may, in some cases, increase the frequency and magnitude of internal P loading during short periods of anoxia. In P limited systems, the apparent ecological benefits of decreased NO_3^- may be offset by increased P release and eutrophication. However, numerous additional processes exist in natural systems, which were not simulated during our reactor experiment and may influence internal loading mechanisms. Finally, we demonstrate that oscillatory redox conditions, even in sediments with diverse and active microbial communities, do not necessarily result in accumulation of polyphosphate, due to

Chris Parsons 2017-5-4 17:10
Deleted: short chain fatty acids

Chris Parsons 2017-4-30 12:53
Deleted: Implications

Chris Parsons 2017-4-30 12:54
Formatted: Heading 1, Line spacing: single

Chris Parsons 2017-4-30 12:48
Deleted: coupling

Chris Parsons 2017-4-30 12:55
Deleted:

Chris Parsons 2017-4-30 12:54
Deleted:

Chris Parsons 2017-5-4 14:59
Deleted: the management of

Chris Parsons 2017-4-30 02:05
Deleted: WWTP effluent

Chris Parsons 2017-4-30 02:06
Deleted: WWTP effluent

Chris Parsons 2017-5-3 14:15
Deleted:

Chris Parsons 2017-4-30 02:06
Deleted: ostensibly

mineralogical phosphate immobilization and scavenging of SCFA by anaerobic heterotrophic respiration.

Funding Sources

We acknowledge funding from the Canadian Excellence Research Chair (CERC) program and the Water Institute at the University of Waterloo.

Acknowledgements

We would like to acknowledge the support of the Royal Botanical Gardens, particularly Jennifer Bowman and Tys Theymeyer as well as Taylor Maavara who kindly provided her pack raft for use during field sampling. We also acknowledge Jia Cheng (Allen) Yu for his assistance with the production of Figure 1 as well as Marianne Vandergriendt, Kassandra Ma and Christine Ridenour for laboratory assistance.

Chris Parsons 2017-4-30 12:56
Deleted: ,

Chris Parsons 2017-4-30 02:07
Deleted: .

Abbreviations

Green filamentous algae; GFA, waste water treatment plants; WWTP, sediment-water interface; SWI, dissolved organic carbon; DOC, organic phosphorus species; P_o, soluble reactive phosphorus; SRP, Inductively Coupled Plasma Optical Emission Spectrometry; ICP-OES, organic matter; OM, powder X-ray diffraction; XRD, dissolved reactive phosphorus; DRP, Method detection limit; MDL, non-purgeable organic carbon; NPOC, total dissolved phosphorus; TDP, dissolved inorganic carbon; DIC, relative standard deviation; RSD%, 4-methylumbelliferyl; MUF, 4-Methylumbelliferyl phosphate; MUP, Bis(4-methylumbelliferyl)phosphate; DiMUP, and 4-Methylumbelliferyl pyrophosphate; PYRO-P, 4-

Methylumbelliferyl beta-D-glucopyranoside; MUGb, thermo-gravimetric analysis; TGA, terminal electron acceptors; TEAs, particulate organic matter; POM, total phosphorus; TP.

References

4500-P E: Phosphorus by Ascorbic Acid, 1992. , Standard Methods for the Examination of Water and Wastewater. National Water Quality Monitoring Council, Washington, DC, U.S.

Aller, R.C., 2004. Conceptual models of early diagenetic processes: The muddy seafloor as an unsteady, batch reactor. J. Mar. Res. 62, 815–835. doi:10.1357/0022240042880837

Aller, R.C., 1994. Bioturbation and remineralization of sedimentary organic matter: effects of redox oscillation. Chem. Geol. 114, 331–345. doi:doi: 10.1016/0009-2541(94)90062-0

Amirbahman, A., Lake, B.A., Norton, S.A., 2013. Seasonal phosphorus dynamics in the surficial sediment of two shallow temperate lakes: a solid-phase and pore-water study. Hydrobiologia 701, 65–77. doi:10.1007/s10750-012-1257-z

Baldwin, D.S., 1996. The phosphorus composition of a diverse series of Australian sediments. Hydrobiologia 335, 63–73. doi:10.1007/BF00013684

Berner, R.A., 1977. Stoichiometric models for nutrient regeneration m anoxic sediments1: Nutrient regeneration. Limnol. Oceanogr. 22, 781–786. doi:10.4319/lo.1977.22.5.0781

Bonneville, S., Van Cappellen, P., Behrends, T., 2004. Microbial reduction of iron(III) oxyhydroxides: effects of mineral solubility and availability. Chem. Geol. 212, 255–268. doi:doi: 10.1016/j.chemgeo.2004.08.015

Bowman, J., Theysmeyer, T., 2014. 2013 RBG Marsh Sediment Quality Assessment (No. Report No. 2014-14). Royal Botanical Gardens, Burlington, Ontario.

Cade-Menun, B., 2005. Characterizing phosphorus in environmental and agricultural samples by 31P nuclear magnetic resonance spectroscopy. Talanta 66, 359–371. doi:10.1016/j.talanta.2004.12.024

Cade-Menun, B.J., Carter, M.R., James, D.C., Liu, C.W., 2010. Phosphorus forms and chemistry in the soil profile under long-term conservation tillage: a phosphorus-31 nuclear magnetic resonance study. J. Environ. Qual. 39, 1647–1656.

Cade-Menun, B.J., Navaratnam, J.A., Walbridge, M.R., 2006. Characterizing Dissolved and Particulate Phosphorus in Water with ^{31} P Nuclear Magnetic Resonance Spectroscopy. Environ. Sci. Technol. 40, 7874–7880. doi:10.1021/es061843e

Cade-Menun, B.J., Preston, C.M., 1996. A Comparison of Soil Extraction Procedures for 31P NMR Spectroscopy. Soil Sci. 161, 770–785. doi:10.1097/00010694-199611000-00006

Caldeira, C.L., Ciminelli, V.S.T., Osseo-Asare, K., 2010. The role of carbonate ions in pyrite oxidation in aqueous systems. Geochim. Cosmochim. Acta 74, 1777–1789. doi:doi: 10.1016/j.gca.2009.12.014

Caraco, N.F., Cole, J.J., Likens, G.E., 1989. Evidence for sulphate-controlled phosphorus release from sediments of aquatic systems. Nature 341, 316–318. doi:10.1038/341316a0

Chorover, J., Amistadi, M.K., 2001. Reaction of forest floor organic matter at goethite, birnessite and smectite surfaces. Geochim. Cosmochim. Acta 65, 95–109. doi:10.1016/S0016-7037(00)00511-1

Chris Parsons 2017-5-5 10:59
Formatted: Bibliography, Widow/Orphan control, Adjust space between Latin and Asian text, Adjust space between Asian text and numbers

Unknown
Field Code Changed

Chris Parsons 2017-4-25 10:46
Deleted: 4500-P E: Phosphorus by Ascorbic Acid, 1992. , Standard Methods for the Examination of Water and Wastewater. National Water Quality Monitoring Council, Washington, DC, U.S. ... [19]

Chow-Fraser, P., Lougheed, V., Le Thiec, V., Crosbie, B., Simser, L., Lord, J., 1998. Long-term response of the biotic community to fluctuating water levels and changes in water quality in Cootes Paradise Marsh, a degraded coastal wetland of Lake Ontario. Wetl. Ecol. Manag. 6, 19–42. doi:10.1023/A:1008491520668

Chun, C.L., Ochsner, U., Byappanahalli, M.N., Whitman, R.L., Tepp, W.H., Lin, G., Johnson, E.A., Peller, J., Sadowsky, M.J., 2013. Association of Toxin-Producing *Clostridium botulinum* with the Macroalga *Cladophora* in the Great Lakes. Environ. Sci. Technol. 47, 2587–2594. doi:10.1021/es304743m

Cline, J.D., 1969. Spectrophotometric determination of hydrogen sulfide in natural waters. Limnol. Oceanogr. 14, 454–458. doi:10.4319/lo.1969.14.3.0454

Conley, D.J., Paerl, H.W., Howarth, R.W., Boesch, D.F., Seitzinger, S.P., Havens, K.E., Lancelot, C., Likens, G.E., 2009. ECOLOGY: Controlling Eutrophication: Nitrogen and Phosphorus. Science 323, 1014–1015. doi:10.1126/science.1167755

Corazza, C., Tironi, S., 2011. European Parliament supports ban of phosphates in consumer detergents (Press Release No. IP/11/1542). European Commission, Brussels, Belgium.

D. Krom, M., A. Berner, R., 1981. The diagenesis of phosphorus in a nearshore marine sediment. Geochim. Cosmochim. Acta 45, 207–216. doi:10.1016/0016-7037(81)90164-2

DeAngelis, K.M., Silver, W.L., Thompson, A.W., Firestone, M.K., 2010. Microbial communities acclimate to recurring changes in soil redox potential status. Environ. Microbiol. 12, 3137–3149. doi:10.1111/j.1462-2920.2010.02286.x

Deng, S., Popova, I.E., Dick, L., Dick, R., 2013. Bench scale and microplate format assay of soil enzyme activities using spectroscopic and fluorometric approaches. Appl. Soil Ecol. 64, 84–90. doi:10.1016/j.apsoil.2012.11.002

Doolette, A.L., Smernik, R.J., Dougherty, W.J., 2009. Spiking Improved Solution Phosphorus-31 Nuclear Magnetic Resonance Identification of Soil Phosphorus Compounds. Soil Sci. Soc. Am. J. 73, 919. doi:10.2136/sssaj2008.0192

Dunn, C., Jones, T.G., Girard, A., Freeman, C., 2013. Methodologies for Extracellular Enzyme Assays from Wetland Soils. Wetlands 34, 9–17. doi:10.1007/s13157-013-0475-0

Einsele, W., 1936. Über die Beziehungen des Eisenkreislaufs zum Phosphatkreislauf im eutrophen See. Arch Hydrobiol 29, 664–686.

Fisher, J.B., Lick, W.J., McCall, P.L., Robbins, J.A., 1980. Vertical mixing of lake sediments by tubificid oligochaetes. J. Geophys. Res. 85, 3997. doi:10.1029/JC085iC07p03997

Frohne, T., Rinklebe, J., Diaz-Bone, R.A., Du Laing, G., 2011. Controlled variation of redox conditions in a floodplain soil: Impact on metal mobilization and biomethylation of arsenic and antimony. Geoderma 160, 414–424. doi:doi:10.1016/j.geoderma.2010.10.012

Furukawa, Y., Bentley, S.J., Lavoie, D.L., 2001. Bioirrigation modeling in experimental benthic mesocosms. J. Mar. Res. 59, 417–452. doi:10.1357/002224001762842262

Gächter, R., Meyer, J.S., 1993. The role of microorganisms in mobilization and fixation of phosphorus in sediments. Hydrobiologia 253, 103–121. doi:10.1007/BF00050731

Gächter, R., Meyer, J.S., Mares, A., 1988. Contribution of bacteria to release and fixation of phosphorus in lake sediments: Bacteria and P in sediments. Limnol. Oceanogr. 33, 1542–1558. doi:10.4319/lo.1988.33.6part2.1542

Gächter, R., Müller, B., 2003. Why the Phosphorus Retention of Lakes Does Not Necessarily Depend on the Oxygen Supply to Their Sediment Surface. Limnol. Oceanogr. 48, 929–933. doi:10.2307/3096591

Gardner, W.H., 1986. Water Content, in: Methods of Soil Analysis: Physical and Mineralogical Methods, Agronomy. Soil Science Society of America, Madison, Wisconsin, pp. 493–544.
Gehin, A., Greneche, J.-M., Tournassat, C., Brendle, J., Rancourt, D.G., Charlet, L., 2007. Reversible surface-sorption-induced electron-transfer oxidation of Fe(II) at reactive sites on a synthetic clay mineral. Geochim. Cosmochim. Acta 71, 863–876. doi:doi: 10.1016/j.gca.2006.10.019
Gerke, J., 2010. Humic (Organic Matter)-Al(Fe)-Phosphate Complexes: An Underestimated Phosphate Form in Soils and Source of Plant-Available Phosphate. Soil Sci. 175, 417–425. doi:10.1097/SS.0b013e3181f1b4dd
Gerke, J., 1993. Phosphate adsorption by humic/Fe-oxide mixtures aged at pH 4 and 7 and by poorly ordered Fe-oxide. Geoderma 59, 279–288. doi:10.1016/0016-7061(93)90074-U
Gorham, E., Boyce, F.M., 1989. Influence of Lake Surface Area and Depth Upon Thermal Stratification and the Depth of the Summer Thermocline. J. Gt. Lakes Res. 15, 233–245. doi:10.1016/S0380-1330(89)71479-9
Grybos, M., Davranche, M., Gruau, G., Petitjean, P., Pedrot, M., 2009. Increasing pH drives organic matter solubilization from wetland soils under reducing conditions. Geoderma 154, 13–19. doi:doi: DOI: 10.1016/j.geoderma.2009.09.001
Hansen, J.C., Cade-Menun, B.J., Strawn, D.G., 2004. Phosphorus Speciation in Manure-Amended Alkaline Soils. J. Environ. Qual. 33, 1521. doi:10.2134/jeq2004.1521
Hedley, M.J., White, R.E., Nye, P.H., 1982. Plant-Induced changes in the rhizosphere of rape (Brassica Napus Var.Emerald) seedlings. III. Changes in L value, soil phosphate fractions and phosphatase activity. New Phytol. 91, 45–56. doi:10.1111/j.1469-8137.1982.tb03291.x
Hölker, F., Vanni, M.J., Kuiper, J.J., Meile, C., Grossart, H.-P., Stief, P., Adrian, R., Lorke, A., Dellwig, O., Brand, A., Hupfer, M., Mooij, W.M., Nützmann, G., Lewandowski, J., 2015. Tube-dwelling invertebrates: tiny ecosystem engineers have large effects in lake ecosystems. Ecol. Monogr. 85, 333–351. doi:10.1890/14-1160.1
Hongve, D., 1997. Cycling of iron, manganese, and phosphate in a meromictic lake. Limnol. Oceanogr. 42, 635–647. doi:10.4319/lo.1997.42.4.0635
Hupfer, M., Gloess, S., Grossart, H., 2007. Polyphosphate-accumulating microorganisms in aquatic sediments. Aquat. Microb. Ecol. 47, 299–311. doi:10.3354/ame047299
Hyacinthe, C., Van Cappellen, P., 2004. An authigenic iron phosphate phase in estuarine sediments: composition, formation and chemical reactivity. Mar. Chem. 91, 227–251. doi:10.1016/j.marchem.2004.04.006
Jensen, D.L., Boddum, J.K., Tjell, J.C., Christensen, T.H., 2002. The solubility of rhodochrosite (MnCO3) and siderite (FeCO3) in anaerobic aquatic environments. Appl. Geochem. 17, 503–511. doi:doi: DOI: 10.1016/S0883-2927(01)00118-4
Jensen, H.S., Kristensen, P., Jeppesen, E., Skytthe, A., 1992. Iron:phosphorus ratio in surface sediment as an indicator of phosphate release from aerobic sediments in shallow lakes. Hydrobiologia 235–236, 731–743. doi:10.1007/BF00026261
Jørgensen, C., Inglett, K.S., Jensen, H.S., Reitzel, K., Reddy, K.R., 2015. Characterization of biogenic phosphorus in outflow water from constructed wetlands. Geoderma 257–258, 58–66. doi:10.1016/j.geoderma.2015.01.019
Joshi, S.R., Kukkadapu, R.K., Burdige, D.J., Bowden, M.E., Sparks, D.L., Jaisi, D.P., 2015. Organic Matter Remineralization Predominates Phosphorus Cycling in the Mid-Bay

Sediments in the Chesapeake Bay. Environ. Sci. Technol. 49, 5887–5896. doi:10.1021/es5059617
Kang, H., Freeman, C., 1999. Phosphatase and arylsulphatase activities in wetland soils: annual variation and controlling factors. Soil Biol. Biochem. 31, 449–454. doi:10.1016/S0038-0717(98)00150-3
Katsev, S., Tsandev, I., L'Heureux, I., Rancourt, D.G., 2006. Factors controlling long-term phosphorus efflux from lake sediments: Exploratory reactive-transport modeling. Chem. Geol. 234, 127–147. doi:10.1016/j.chemgeo.2006.05.001
Kim, D.-K., Zhang, W., Rao, Y.R., Watson, S., Mugalingam, S., Labencki, T., Dittrich, M., Morley, A., Arhonditsis, G.B., 2013. Improving the representation of internal nutrient recycling with phosphorus mass balance models: A case study in the Bay of Quinte, Ontario, Canada. Ecol. Model. 256, 53–68. doi:10.1016/j.ecolmodel.2013.02.017
Kizewski, F.R., Boyle, P., Hesterberg, D., Martin, J.D., 2010a. Mixed Anion (Phosphate/Oxalate) Bonding to Iron(III) Materials. J. Am. Chem. Soc. 132, 2301–2308. doi:10.1021/ja908807b
Kizewski, F.R., Hesterberg, D., Martin, J., 2010b. Phosphate sorption to organic matter/ferrihydrite systems as affected by aging time. Presented at the 19th World Congress of Soil Science, Soil Solutions for a Changing World, Brisbane, Australia.
Klein, A.R., Baldwin, D.S., Singh, B., Silvester, E.J., 2010. Salinity-induced acidification in a wetland sediment through the displacement of clay-bound iron(II). Environ. Chem. 7, 413. doi:10.1071/EN10057
Kortstee, G.J.J., Appeldoorn, K.J., Bonting, C.F.C., Niel, E.W.J., Veen, H.W., 1994. Biology of polyphosphate-accumulating bacteria involved in enhanced biological phosphorus removal. FEMS Microbiol. Rev. 15, 137–153. doi:10.1111/j.1574-6976.1994.tb00131.x
Lagauzère, S., Boyer, P., Stora, G., Bonzom, J.-M., 2009. Effects of uranium-contaminated sediments on the bioturbation activity of Chironomus riparius larvae (Insecta, Diptera) and Tubifex tubifex worms (Annelida, Tubificidae). Chemosphere 76, 324–334. doi:10.1016/j.chemosphere.2009.03.062
Li, W., Joshi, S.R., Hou, G., Burdige, D.J., Sparks, D.L., Jaisi, D.P., 2015. Characterizing Phosphorus Speciation of Chesapeake Bay Sediments Using Chemical Extraction, ^{31}P NMR, and X-ray Absorption Fine Structure Spectroscopy. Environ. Sci. Technol. 49, 203–211. doi:10.1021/es504648d
Liger, E., Charlet, L., Van Cappellen, P., 1999. Surface catalysis of uranium(VI) reduction by iron(II). Geochim. Cosmochim. Acta 63, 2939–2955. doi:doi: DOI: 10.1016/S0016-7037(99)00265-3
Mallin, M.A., McIver, M.R., Wells, H.A., Parsons, D.C., Johnson, V.L., 2005. Reversal of eutrophication following sewage treatment upgrades in the New River Estuary, North Carolina. Estuaries 28, 750–760. doi:10.1007/BF02732912
Manning, B.A., 1996. Modeling Arsenate Competitive Adsorption on Kaolinite, Montmorillonite and Illite. Clays Clay Miner. 44, 609–623. doi:10.1346/CCMN.1996.0440504
Matisoff, G., Kaltenberg, E.M., Steely, R.L., Hummel, S.K., Seo, J., Gibbons, K.J., Bridgeman, T.B., Seo, Y., Behbahani, M., James, W.F., Johnson, L.T., Doan, P., Dittrich, M., Evans, M.A., Chaffin, J.D., 2016. Internal loading of phosphorus in western Lake Erie. J. Gt. Lakes Res. 42, 775–788. doi:10.1016/j.jglr.2016.04.004
Matisoff, G., Wang, X., 1998. Solute transport in sediments by freshwater infaunal bioirrigators. Limnol. Oceanogr. 43, 1487–1499. doi:10.4319/lo.1998.43.7.1487

Mayer, T., Rosa, F., Mayer, R., Charlton, M., 2006. Relationship Between the Sediment Geochemistry and Phosphorus Fluxes in a Great Lakes Coastal Marsh, Cootes Paradise, ON, Canada. Water Air Soil Pollut. Focus 6, 495–503. doi:10.1007/s11267-006-9033-6

McCall, P.L., Fisher, J.B., 1980. Effects of Tubificid Oligochaetes on Physical and Chemical Properties of Lake Erie Sediments, in: Brinkhurst, R., Cook, D. (Eds.), Aquatic Oligochaete Biology. Springer US, pp. 253–317.

McLaughlin, C., Pike, K., 2014. Muddied Waters: The Ongoing Challenge of Sediment and Phosphorus for Hamilton Harbour Remediation (2014 Towards Safe Harbour Report). Bay Area Restoration Council, Hamilton, Ontario.

Mikutta, C., Kretzschmar, R., 2011. Spectroscopic Evidence for Ternary Complex Formation between Arsenate and Ferric Iron Complexes of Humic Substances. Environ. Sci. Technol. 45, 9550–9557. doi:10.1021/es202300w

Mortimer, C.H., 1971. Chemical Exchanges Between Sediments and Water in the Great Lakes-Speculations on Probable Regulatory Mechanisms. Limnol. Oceanogr. 16, 387–404. doi:10.2307/2834170

Mortimer, C.H., 1941. The exchange of dissolved substances between mud and water in lakes. J. Ecol. 29, 280–329.

Murphy, J., Riley, J.P., 1962. A modified single solution method for the determination of phosphate in natural waters. Anal. Chim. Acta 27, 31–36. doi:10.1016/S0003-2670(00)88444-5

Nikolausz, M., Kappelmeyer, U., Szekely, A., Rusznyak, A., Marialigeti, K., Kastner, M., 2008. Diurnal redox fluctuation and microbial activity in the rhizosphere of wetland plants. Eur. J. Soil Biol. 44, 324–333. doi:doi: DOI: 10.1016/j.ejsobi.2008.01.003

Nürnberg, G.K., 1988. Prediction of Phosphorus Release Rates from Total and Reductant-Soluble Phosphorus in Anoxic Lake Sediments. Can. J. Fish. Aquat. Sci. 45, 453–462. doi:10.1139/f88-054

O'Connell, D.W., Jensen, M.M., Jakobsen, R., Thamdrup, B., Andersen, T.J., Kovacs, A., Hansen, H.C.B., 2015. Vivianite formation and its role in phosphorus retention in Lake Ørn, Denmark. Chem. Geol. doi:10.1016/j.chemgeo.2015.05.002

Olsen, S.R., Cole, C.V., Watanabe, F.S., Dean, L.A., 1954. Estimation of available phosphorus in soils by extraction with sodium bicarbonate. US Dep Agric Circ 939, 1–19.

Olsen, S.R., Watanabe, F.S., 1957. A Method to Determine a Phosphorus Adsorption Maximum of Soils as Measured by the Langmuir Isotherm1. Soil Sci. Soc. Am. J. 21, 144. doi:10.2136/sssaj1957.03615995002100020004x

Painter, D.., Hampton, L., Simser, W.L., 1991. Cootes Paradise Water Turbidity: Sources and Recommendations., in: NWRI Contribution Paper #91-15. Burlington, Ontario, p. 18.

Pallasser, R., Minasny, B., McBratney, A.B., 2013. Soil carbon determination by thermogravimetrics. PeerJ 1, e6. doi:10.7717/peerj.6

Paraskova, J.V., Jørgensen, C., Reitzel, K., Pettersson, J., Rydin, E., Sjöberg, P.J.R., 2015. Speciation of Inositol Phosphates in Lake Sediments by Ion-Exchange Chromatography Coupled with Mass Spectrometry, Inductively Coupled Plasma Atomic Emission Spectroscopy, and ^{31}P NMR Spectroscopy. Anal. Chem. 87, 2672–2677. doi:10.1021/ac5033484

Parkhurst, D.L., Appelo, C.A.J., (US), G.S., 1999. User's guide to PHREEQC (Version 3): A computer program for speciation, batch-reaction, one-dimensional transport, and inverse geochemical calculations. US Geological Survey Reston, VA.

Parsons, C.T., Couture, R.-M., Omoregie, E.O., Bardelli, F., Greneche, J.-M., Roman-Ross, G., Charlet, L., 2013. The impact of oscillating redox conditions: Arsenic immobilisation in contaminated calcareous floodplain soils. Environ. Pollut. 178, 254–263. doi:10.1016/j.envpol.2013.02.028

Peiffer, S., Behrends, T., Hellige, K., Larese-Casanova, P., Wan, M., Pollok, K., 2015. Pyrite formation and mineral transformation pathways upon sulfidation of ferric hydroxides depend on mineral type and sulfide concentration. Chem. Geol. 400, 44–55. doi:10.1016/j.chemgeo.2015.01.023

Pelegri, S.P., Blackburn, T.H., 1995. Effects of Tubifex tubifex (Oligochaeta: Tubificidae) on N-mineralization in freshwater sediments, measured with isotopes. Aquat. Microb. Ecol. 9, 289–294.

Penn, M.R., Auer, M.T., Doerr, S.M., Driscoll, C.T., Brooks, C.M., Effler, S.W., 2000. Seasonality in phosphorus release rates from the sediments of a hypereutrophic lake under a matrix of pH and redox conditions. Can. J. Fish. Aquat. Sci. 57, 1033–1041. doi:10.1139/f00-035

Phillips, G., Jackson, R., Bennett, C., Chilvers, A., 1994. The importance of sediment phosphorus release in the restoration of very shallow lakes (The Norfolk Broads, England) and implications for biomanipulation. Hydrobiologia 275–276, 445–456. doi:10.1007/BF00026733

Pomeroy, R., 1954. Auxiliary Pretreatment by Zinc Acetate in Sulfide Analyses. Anal. Chem. 26, 571–572. doi:10.1021/ac60087a047

Pretty, J.N., Mason, C.F., Nedwell, D.B., Hine, R.E., Leaf, S., Dils, R., 2003. Environmental Costs of Freshwater Eutrophication in England and Wales. Environ. Sci. Technol. 37, 201–208. doi:10.1021/es020793k

Reddy, K.R., DeLaune, R.D., 2008. Biogeochemistry of wetlands: science and applications. CRC Press, Boca Raton.

Reddy, K.R., Newman, S., Osborne, T.Z., White, J.R., Fitz, H.C., 2011. Phosphorous Cycling in the Greater Everglades Ecosystem: Legacy Phosphorous Implications for Management and Restoration. Crit. Rev. Environ. Sci. Technol. 41, 149–186. doi:10.1080/10643389.2010.530932

Reitzel, K., Ahlgren, J., DeBrabandere, H., Waldebäck, M., Gogoll, A., Tranvik, L., Rydin, E., 2007. Degradation rates of organic phosphorus in lake sediment. Biogeochemistry 82, 15–28. doi:10.1007/s10533-006-9049-z

Rezanezhad, F., Couture, R.-M., Kovac, R., O'Connell, D., Van Cappellen, P., 2014. Water table fluctuations and soil biogeochemistry: An experimental approach using an automated soil column system. J. Hydrol. 509, 245–256. doi:10.1016/j.jhydrol.2013.11.036

Rickard, D., Morse, J.W., 2005. Acid volatile sulfide (AVS). Mar. Chem. 97, 141–197. doi:10.1016/j.marchem.2005.08.004

Routledge, I., 2012. City of Hamilton: King Street (Dundas) Wastewater Treatment Plant. 2011 Annual Report (Annual Report No. Works Number 120001372). The City of Hamilton, Environment and Sustainable Infrastructure Division, Hamilton, Ontario.

Ruttenberg, K.C., 1992. Development of a sequential extraction method for different forms of phosphorus in marine sediments. Limnol. Oceanogr. 37, 1460–1482. doi:10.4319/lo.1992.37.7.1460

Sannigrahi, P., Ingall, E., 2005. Polyphosphates as a source of enhanced P fluxes in marine sediments overlain by anoxic waters: Evidence from [sup 31]P NMR. Geochem. Trans. 6, 52. doi:10.1063/1.1946447

Semkin, R.G., McLarty, A.W., Craig, D., 1976. A water quality study of Cootes Paradise. Ontario Ministry of Environment, West Central Region, Toronto, Ontario.

Sharma, P., Ofner, J., Kappler, A., 2010. Formation of Binary and Ternary Colloids and Dissolved Complexes of Organic Matter, Fe and As. Environ. Sci. Technol. 44, 4479–4485. doi:10.1021/es100066s

Sharpley, A.N., Chapra, S.C., Wedepohl, R., Sims, J.T., Daniel, T.C., Reddy, K.R., 1994. Managing Agricultural Phosphorus for Protection of Surface Waters: Issues and Options. J. Environ. Qual. 23, 437. doi:10.2134/jeq1994.00472425002300030006x

Sibanda, H.M., Young, S.D., 1986. Competitive adsorption of humus acids and phosphate on goethite, gibbsite and two tropical soils. J. Soil Sci. 37, 197–204. doi:10.1111/j.1365-2389.1986.tb00020.x

Sirová, D., Rejmánková, E., Carlson, E., Vrba, J., 2013. Current standard assays using artificial substrates overestimate phosphodiesterase activity. Soil Biol. Biochem. 56, 75–79. doi:10.1016/j.soilbio.2012.02.008

Smith, V.H., Schindler, D.W., 2009. Eutrophication science: where do we go from here? Trends Ecol. Evol. 24, 201–207. doi:10.1016/j.tree.2008.11.009

Søndergaard, M., Jensen, J.P., Jeppesen, E., 2003. Role of sediment and internal loading of phosphorus in shallow lakes. Hydrobiologia 506–509, 135–145. doi:10.1023/B:HYDR.0000008611.12704.dd

Song, K.-Y., Zoh, K.-D., Kang, H., 2007. Release of phosphate in a wetland by changes in hydrological regime. Sci. Total Environ. 380, 13–18. doi:10.1016/j.scitotenv.2006.11.035

Stookey, L.L., 1970. Ferrozine - a new spectrophotometric reagent for iron. Anal. Chem. 42, 779–781. doi:doi: 10.1021/ac60289a016

Stumm, W., Morgan, J.J., 1996. Aquatic Chemistry, 3rd ed. ed. John Wiley & Sons, New York [etc.].

Theysmeyer, T., Smith, T., Simser, L., 1999. West Pond 1999 Study. Royal Botanical Gardens, Science Department.

Thibault, P.-J., Rancourt, D.G., Evans, R.J., Dutrizac, J.E., 2009. Mineralogical confirmation of a near-P:Fe=1:2 limiting stoichiometric ratio in colloidal P-bearing ferrihydrite-like hydrous ferric oxide. Geochim. Cosmochim. Acta 73, 364–376. doi:10.1016/j.gca.2008.10.031

Thompson, A., Chadwick, O.A., Rancourt, D.G., Chorover, J., 2006. Iron-oxide crystallinity increases during soil redox oscillations. Geochim. Cosmochim. Acta 70, 1710–1727. doi:10.1016/j.gca.2005.12.005

Turner, B.L., Cade-Menun, B.J., Westermann, D.T., 2003a. Organic phosphorus composition and potential bioavailability in semi-arid arable soils of the Western United States. Soil Sci. Soc. Am. J. 67, 1168–1179.

Turner, B.L., Mahieu, N., Condron, L., 2003b. Phosphorus-31 Nuclear Magnetic Resonance Spectral Assignments of Phosphorus Compounds in Soil NaOH–EDTA Extracts. Soil Sci. Soc. Am. J. 67, 497. doi:10.2136/sssaj2003.4970

U.S. EPA, 9/99. Field Sampling Guidance Document: Sediment Sampling (No. #1215). U.S. Environmental Protection Agency. Region 9 Laboratory, Richmond California.

Vetter, Y.A., Deming, J.W., Jumars, P.A., Krieger-Brockett, B.B., 1998. A Predictive Model of Bacterial Foraging by Means of Freely Released Extracellular Enzymes. Microb. Ecol. 36, 75–92. doi:10.1007/s002489900095

Viollier, E., Inglett, P.., Hunter, K., Roychoudhury, A.., Van Cappellen, P., 2000. The ferrozine method revisited: Fe(II)/Fe(III) determination in natural waters. Appl. Geochem. 15, 785–790. doi:10.1016/S0883-2927(99)00097-9

Weishaar, J.L., Aiken, G.R., Bergamaschi, B.A., Fram, M.S., Fujii, R., Mopper, K., 2003. Evaluation of Specific Ultraviolet Absorbance as an Indicator of the Chemical Composition and Reactivity of Dissolved Organic Carbon. Environ. Sci. Technol. 37, 4702–4708. doi:10.1021/es030360x

Wentzel, M.C., Lötter, L.H., Ekama, G.A., Loewenthal, R.E., Marais, G. v R., 1991. Evaluation of Biochemical Models for Biological Excess Phosphorus Removal. Water Sci. Technol. 23, 567–576.

Yamamoto-Ikemoto, R., Matsui, S., Komori, T., 1994. Ecological interactions among denitrification, poly-P accumulation, sulfate reduction, and filamentous sulfur bacteria in activated sludge. Water Sci. Technol. 30, 201–210.

Chris Parsons 2017-5-3 14:00
Formatted: Heading 1

Tables

Step	Extractant	Conditions	Target phase
1a	1M $MgCl_2$	pH 8 for 2 hours @ 25ºC	Exchangeable or Loosely sorbed P (P_{Ex})
1b	1M $MgCl_2$	pH 8 for 2 hours @ 25ºC	
1c	18.2 MΩ cm^{-1} H_2O	2 hours @ 25ºC	
2a	1M $NaHCO_3$	pH 7.6 for 16 hours @ 25ºC	Organic associated P (P_{Hum})
2b	1M $NaHCO_3$	pH 7.6 for 2 hours @ 25ºC	
2c	1M $NaHCO_3$	pH 7.6 for 2 hours @ 25ºC	
2d	1M $NaHCO_3$	pH 7.6 for 2 hours @ 25ºC	
2e	1M $MgCl_2$	pH 8 for 2 hours @ 25ºC	
3a	0.3 M Na_3-citrate with 1M $NaHCO_3$ with 1.125g of Na-ditionite (CDB)	pH 7.6 for 8 hours @ 25ºC	Fe-bound P (P_{Fe})
3b	CDB	pH 7.6 for 2 hours @ 25ºC	
3c	1M $MgCl_2$	pH 8 for 2 hours @ 25ºC	
4a	1M Na-acetate with acetic acid	pH 4 for 6 hours @ 25ºC	Authigenic carbonate fluorapatite plus biogenic apatite plus $CaCO_3$-bound P (P_{CFA})
4b	1M Na-acetate with acetic acid	pH 4 for 2 hours @ 25ºC	
4c	1M $MgCl_2$	pH 8 for 2 hours @ 25ºC	
5	1M HCl	16 hours @ 25ºC	Detrital Apatite plus other inorganic-P (P_{Detri})

6	1M HCl	16 hours after ashing at 550°C @ 25°C	Residual/Organic-P (P_{Resi})

Table 1: Summary of the modified SEDEX sequential extraction protocol used on solid samples taken over a time series during the reactor experiment. Results of this extraction are shown in Figure 4.

Figures

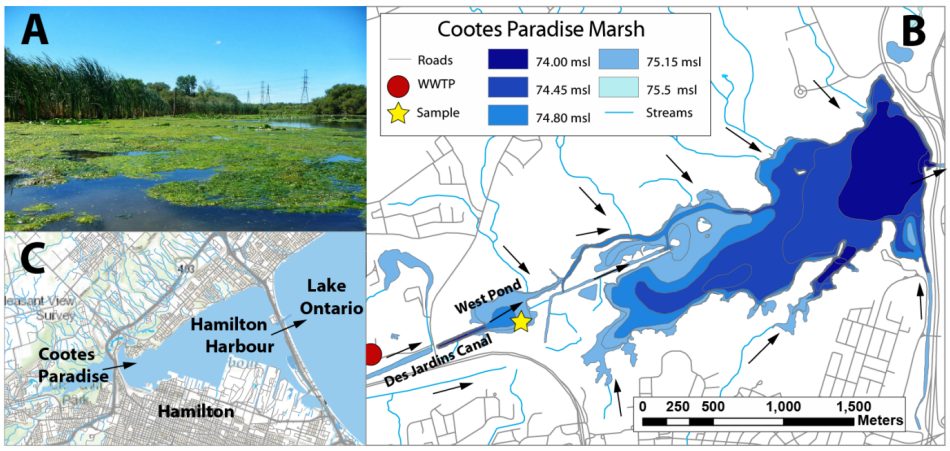

Figure 1: A) Photograph of the sampling location taken on the day of sampling illustrating the abundance of green filamentous algae. B) Map of Cootes Paradise and West Pond showing the sampling location, local hydrological network and the King Street Waste Water Treatment plant in Dundas. Color represents area covered by surface water at different water levels (msl= meters above sea level) C) Overview map showing the hydrological connection between Cootes Paradise, Hamilton Harbour and Lake Ontario.

Chris Parsons 2017-5-3 14:01
Formatted: Keep with next

Chris Parsons 2017-5-3 14:03
Formatted: Caption, Line spacing: double

Chris Parsons 2017-5-5 11:39
Formatted: Subtle Emphasis, Font:+Theme Headings, Font color: Text 1, Expanded by 0.75 pt

Chris Parsons 2017-5-5 11:39
Formatted: Font:12 pt, Not Bold, Font color: Text 1, Expanded by 0.75 pt

Chris Parsons 2017-5-4 00:31
Formatted: Subtle Emphasis, Font:+Theme Headings, Font color: Text 1, Expanded by 0.75 pt

Chris Parsons 2017-5-3 14:04
Formatted: Font:(Default) +Theme Headings, Expanded by 0.75 pt

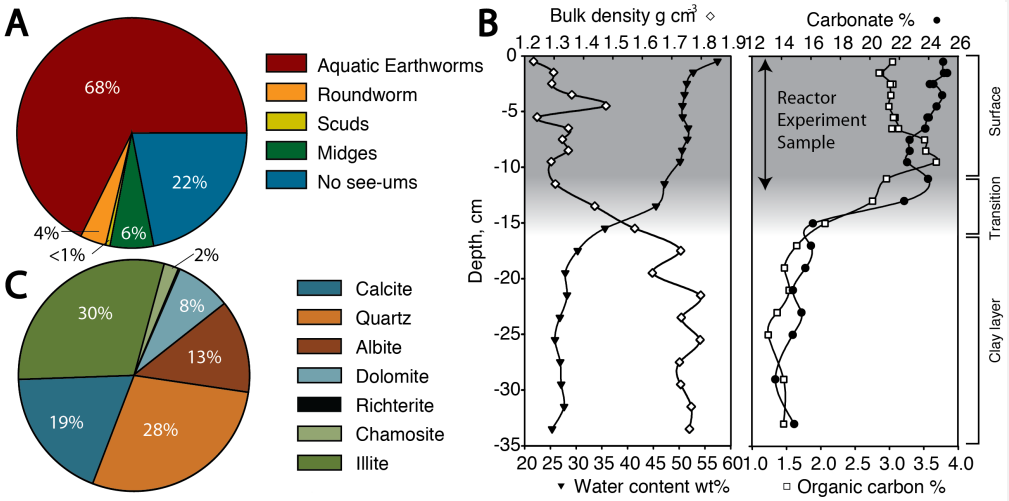

Figure 2: a) Proportions of bioturbating macro invertebrates identified in the top 18 cm b) Depth profiles of sampled sediment, water content weight % (inverted black triangles), bulk density (white diamonds) OM % (white squares), carbonate % (black circles) c) Mineralogical composition of sediments from the zone of bioturbation determined by XRD (top 12 cm).

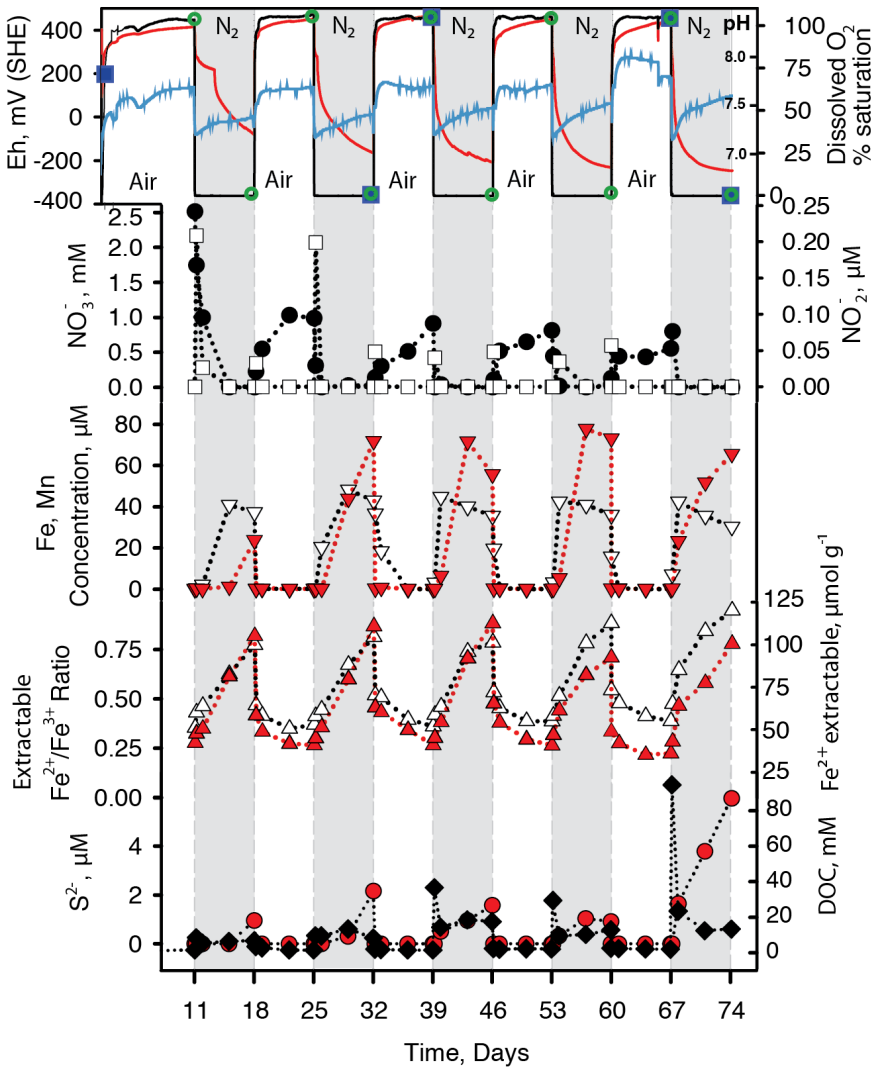

1437

1438 *Figure 3: Aqueous chemistry and iron extraction data with time during reactor*

1439 *experiments: Solid red line = E_h, solid black line = DO, solid blue line = pH, full*

1440 *black circles = NO_3^-, white squares = NO_2^-, inverted red triangles = $Fe_{(aq)}$, inverted*

1441 *white triangles = $Mn_{(aq)}$, red triangles = Fe^{2+} 0.5M HCl extractable, white triangles*

1442 *= Fe^{2+}/Fe^{3+} ratio in 0.5M HCl extract, red circles = S_2^-, black diamonds = DOC.*

1443 *Sampling points for ^{31}P NMR and extracellular enzyme assays (EEA) are shown on*

1444 *the E_h curve (^{31}P NMR = open blue squares, EEA = open green circles).*

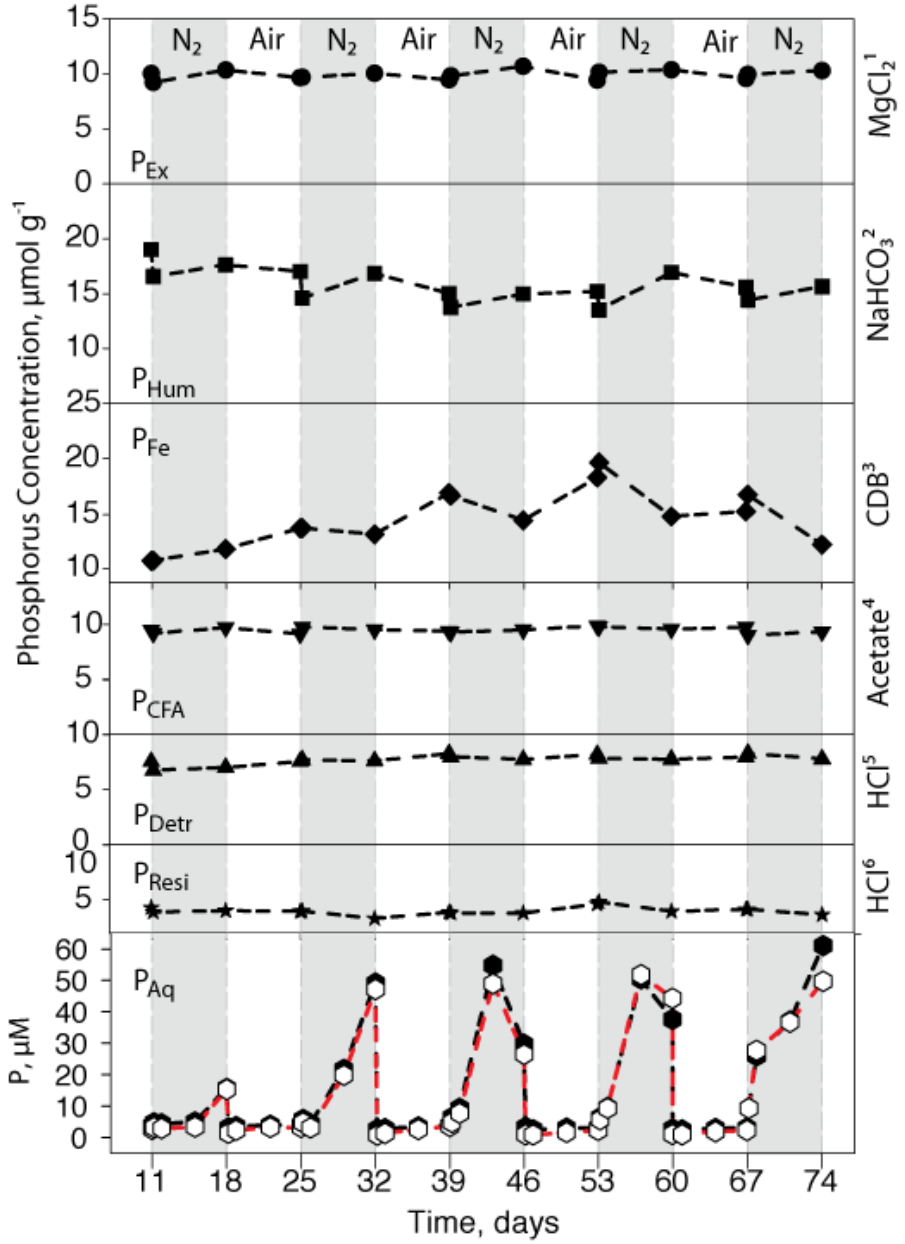

Figure 4: Aqueous and solid phase phosphorus speciation from sequential chemical extractions with time during the reactor experiment. White panels

correspond to time periods with air sparging, grey panels correspond to time periods with N_2:CO_2 sparging. Black symbols = total P concentration, white symbols = SRP concentration.

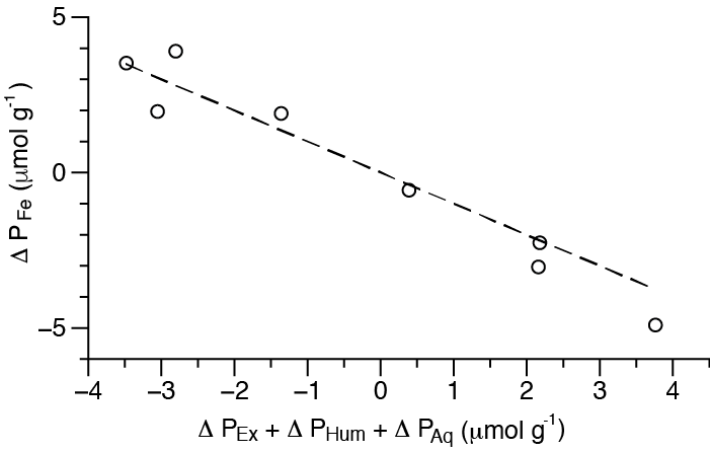

Figure 5: Change in P distribution between the start and end of each oxic and anoxic period (7 day change). Iron-bound P (P_{Fe}) appears to be reversibly redistributed to the loosely sorbed (P_{Ex}), humic bound (P_{Hum}) and aqueous fractions (P_{Aq}). The dashed line is 1:1. Linear regression of the data results in an R^2 of 0.95, a slope of -1.1 and $p < 0.0001$).

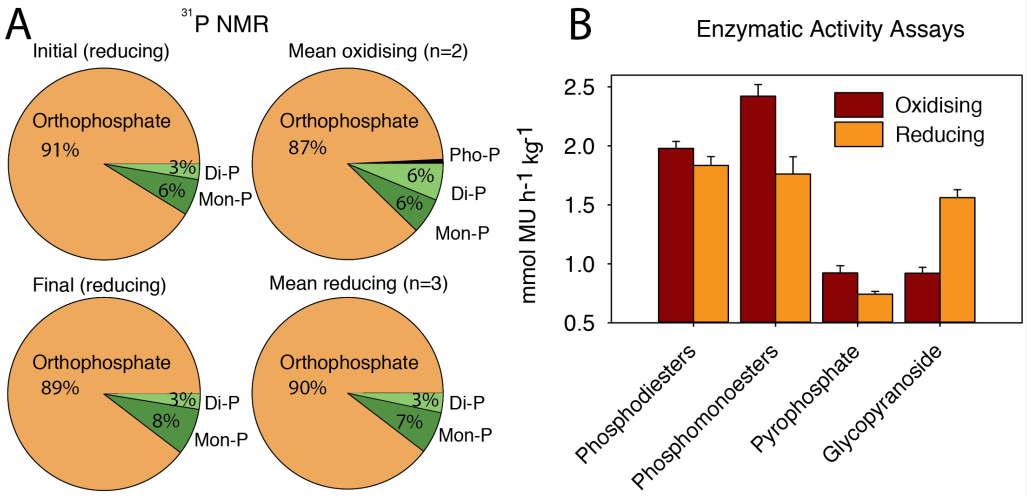

Figure 6: A) P speciation determined by ^{31}P NMR for the initial suspension (top left), the final suspension (bottom left), the average of samples from oxic conditions n=2 (top right), the average of samples from anoxic conditions n=3 (bottom right). Pho-P = phosphonates, Di-P = diester-P, Mon-P = monoester-P. Polyphosphate was not detected at concentrations >1% in any of the samples analyzed. B) Average extracellular enzyme activities under oxic and anoxic conditions for MUP, DiMUP, PYRO-P and MUGb (n=5)